- Title: Positive response of tree productivity to warming is reversed by increased tree density at the Arctic tundra-taiga ecotone
- 3
- 4 **Running head:** Density decreases tree productivity at treeline 5
- 6 **Walker, X.J.**¹ Alexander, H.D.² Berner, L.T.³ Boyd, M.A.⁴ Loranty, M.M.⁵ Natali, S.M.⁶ Mack,
- 7 M.C.⁷
- 8 ¹ Center for Ecosystem Science and Society, Northern Arizona University, Flagstaff, Arizona,
- 9 USA. Email: xanthe.walker@gmail.com
- ² School of Forestry and Wildlife Sciences, Auburn University, Auburn, AL, USA. Email:
- 11 heather.alexander@auburn.edu
- ³ School of Informatics, Computing and Cyber Systems, Northern Arizona University, Flagstaff,
- 13 Arizona, USA. Email: logan.berner@nau.edu
- ⁴ Center for Ecosystem Science and Society, Northern Arizona University, Flagstaff, Arizona,
- 15 USA. Email: melissa.boyd@nau.edu
- ⁵ Department of Geography, Colgate University, Hamilton, New York, USA. Email:
- 17 mloranty@colgate.edu
- ⁶ Woods Hole Research Center, Falmouth, Massachusetts, USA. Email: snatali@whrc.org
- ⁷ Center for Ecosystem Science and Society, Northern Arizona University, Flagstaff, Arizona,
- 20 USA. Email: michelle.mack@nau.edu
- 22 Author contributions: XJW and MCM conceived the study. HDA, MML, SMN, and MCM
- established the sites. HDA, SMN, MML, and MAB collected the field data and MAB completed
- the laboratory work. LTB supplied the NDVI data. XJW analyzed the data and wrote the
- 25 manuscript. All co-authors read and edited the manuscript.
- 27 Data accessibility: Data has been archived in the Arctic Data Center doi:10.18739/A2PC2T79B
- under the parent dataset: urn:uuid:2540d6d2-ea15-4b80-b42e-7bb343090af4. R code used for
- 29 statistical analyses can be found at https://github.com/xanthewalker/Siberia density treering

Abstract

30

31

32

33

34

35

36

37

38

39

40

41

42

43

44

45

46

47

48

49

The transition zone between the northern boreal forest and the arctic tundra, known as the tundra-taiga ecotone (TTE) has undergone rapid warming in recent decades. In response to this warming, tree density, growth, and stand productivity are expected to increase. Increases in tree density have the potential to negate the positive impacts of warming on tree growth through a reduction in the active layer and an increase in competitive interactions. We assessed the effects of tree density on tree growth and climate-growth responses of Cajander larch (*Larix cajanderi*) and on trends in the normalized difference vegetation index (NDVI) in the TTE of Northeast Siberia. We examined 19 mature forest stands that all established after a fire in 1940 and ranged in tree density from 300 to 37,000 stems ha-1. High density stands with shallow active layers had lower tree growth, higher stand productivity, and more negative growth responses to growing season temperatures compared to low density stands with deep active layers. Variation in stand productivity across the density gradient was not captured by Landsat derived NDVI, but NDVI did capture annual variations in stand productivity. Our results suggest that the expected increases in tree density following fires at the TTE may effectively limit tree growth and that NDVI is unlikely to capture increasing productivity associated with changes in tree density.

Keywords: larch, boreal, normalized difference vegetation index (NDVI), climate change, competition, Landsat

50

51

52

55

56

57

58

59

60

61

62

63

64

65

66

67

68

69

70

71

72

73

74

75

76

Introduction

Global climate change is expected to alter the structure and composition of vegetation in transition zones between biomes via species range shifts (Lenoir and Svenning 2015). The transition zone between the boreal forest and the arctic tundra, known as the tundra-taiga ecotone (TTE), is the largest ecotone on earth (Callaghan et al. 2002; Montesano et al. 2020). Across the TTE, tree height, cover, density, and biomass generally decline in association with decreasing temperature (Montesano et al. 2020) and a canopy cover <20% is used to delineate the TTE (Ranson et al. 2011). In recent decades, rapid climate change has occurred throughout the TTE and this warming trend is expected to continue at twice the rate of the global average for at least the next century (Arctic Monitoring and Assessment Programme 2017). Vegetation models predict that with continued warming there will be a significant northward advance of forests and treeless gaps in the present TTE will become forested (Zhang et al. 2013; van der Kolk et al. 2016). Changes in the extent or location of the TTE will have widespread impacts on Arctic ecosystems, including wildlife habitat quality, subsistence activities, and infrastructure (Rickbeil et al. 2018). At a global scale the position of the TTE could have important bioclimatic impacts, including a decrease in the albedo of areas currently covered by tundra and an increase in terrestrial carbon sequestration (Pearson et al. 2013; de Wit et al. 2014).

Despite the importance of understanding vegetation change in the Arctic, observations of range shifts in the TTE have been inconsistent (Harsch et al. 2009; Rees et al. 2020). These inconsistent responses between climate warming and range shifts suggest that there are additional non-climatic factors controlling the position of the TTE. Of the non-climatic factors to consider when making predictions of forest expansion, competitive interactions may be particularly important (Wang et al. 2016; Liang et al. 2016). In the TTE, coniferous trees rarely

form closed high density stands and usually occur in scattered groups (Montesano et al. 2020). However, wildfires throughout the TTE are increasing (Veraverbeke et al. 2017) and their effects on post-fire tree establishment (Landhausser and Wein 1993; Brown 2010) can result in the formation of high density stands (Alexander et al. 2012). Increased competition in dense forests decreases individual tree growth (Assmann 1970) and can alter the growth response of trees to climate (Gea-Izquierdo et al. 2009). In the TTE, growth has historically been limited by relatively short, cold, and sometimes dry growing seasons (Nemani et al. 2003). However, as temperatures increase throughout the northern TTE and high density stands establish post-fire, competitive interactions for limited resources are likely to increase and could play an important role in limiting tree growth responses to climate warming.

Increasing productivity associated with warming in parts of the TTE have been identified by both satellite-derived indicators of productivity (e.g., the normalized difference vegetation, NDVI) and tree-ring data (Beck and Goetz 2011; Berner et al. 2011; Bunn et al. 2013). However, there are many complexities with interpreting satellite measures of productivity at high latitudes (Myers-Smith et al. 2020) and competition can be an even more important factor than temperature in tree limiting growth (Gomez-Aparicio et al. 2011). Specifically, competition for limited resources can modulate the growth response of trees to long-term climate variation (Linares et al. 2010); where trees with low competition often show a strong climate signal compared to trees suppressed by competition (Gea-Izquierdo et al. 2009). In the TTE, the impacts of increased tree density could intensify competitive interactions. Increased shading in high density stands reduces active layer thickness (i.e., the seasonal depth of soil thaw) and can subsequently limit access to water and nutrients (Kropp et al. 2019). The effects of shading have also limited the ability of NDVI to capture increases in forest cover in Siberia (Loranty et al.

2018). There is currently little empirical evidence regarding how competitive interactions affect tree growth responses to climate change or if NDVI captures interannual productivity of trees experiencing different levels of competition. Understanding these dynamics is imperative for predicting forest productivity as climate continues to change and for improving the interpretation of satellite-observed trends in productivity.

In this study, we assessed the productivity of Cajander larch (*Larix cajanderi* (Mayr.)) across a range of tree densities that established following a fire that burned in 1940 in the TTE of northeastern Siberia (Table 1). This region is predicted to experience pronounced shifts in the northern boundary of the TTE (Zhang et al. 2013). We used downscaled climate data, measurements of tree radial growth and stand structure, and Landsat derived NDVI to assess temporal trends in seasonal climate parameters from 1980-2011, density dependent tree growth and stand productivity from 1980-2011, and density dependent NDVI from 1999-2011 (Objective 1). We asked if and how tree density impacts: stand and ecosystem characteristics, individual tree growth, stand productivity, and NDVI (Objective 2), tree growth responses to climate (Objective 3), and the ability of NDVI to detect annual stand productivity (Objective 4).

Methods

Study area and field methods

Our study was conducted near the Northeast Science Station (NESS) in Cherskiy, Sakha Republic, Russia in northeastern Siberia (68.74° N, 161.40° E). From 1938-2009 average annual temperatures was -13.0 °C and total annual precipitation was 282 mm yr⁻¹, approximately half of which occurred during summer (Berner et al. 2013). Forests in this region are composed mostly

123

124

125

126

127

128

129

130

131

132

133

134

135

136

137

138

139

140

141

142

143

144

of the deciduous needleleaf conifer Cajander larch (*Larix cajanderi*) (Alexander et al. 2012), which dominate the permafrost zone of eastern Siberia.

In the summers of 2012, 2015, and 2016, we sampled 19 forest stands (Table 1 and Table S1) across a tree density gradient of Cajander larch located ~ 2 km from the NESS. All stands originated with the same regional species pool after a fire in 1941, and ranged in tree density from 300 - 37,000 trees ha⁻¹. Densities are presumed to be driven by differences in soil burn severity, with higher burn severity promoting higher subsequent tree density (Alexander et al. 2018). The stands are even-aged and show little to no evidence of self-thinning, with little woody debris and few standing dead trees. The stands are within ~3 km of each other and overlay carbon-rich yedoma permafrost, have relatively flat relief, and experience the same climate. They are representative of the greater physiognomy of the typical forested area in the region and their close proximity to one another presents an ideal situation for assessing the effects of density on productivity, while holding other ecological variables relatively constant. Each stand consisted of three plots. All plots were at least 30 m apart and consisted of a 30 m length belt transect of variable width. The width of the belt transect ranged from 1 m wide in the stands with the highest tree density to 8 m wide in the stands with the lowest tree density, resulting in total sample area ranging from 30-240 m².

Within each plot, we measured the diameter at breast height (1.4 m above the base; DBH; cm) of every tree ≥1.4 m tall and basal diameter for trees < 1.4 m tall. We calculated stem density (stems ha⁻¹) and basal area (m² ha⁻¹) for each stand and categorized each stand based on tree density (low= 300 to 3500 stems ha⁻¹; medium= 4400 to 8500 stems ha⁻¹, and high = 10,800 to 37,000 stems ha⁻¹). Canopy cover, understory composition and biomass, active layer depth, and soil organic layer depth were measured using the methods outlined in Alexander et al. 2012

and Paulson et al. in press. Allometric equations were used to calculate C pools of larch trees (Alexander et al. 2012) and tall shrubs (Berner et al. 2012) and C pools of understory vegetation was determined through harvest (Paulson et al. in press). The C of trees, shrubs, and understory vegetation were summed to estimate the total aboveground C pool.

Within each stand, we sampled five to 10 larch trees, obtaining basal cores or disks \sim 30 cm above the forest floor, for tree ring analysis. For stands with 10 trees sampled, we sampled the closest tree located 5m to the left of the 0, 15, and 30 m mark in each of the three plots. The 10^{th} tree was sampled 5 m to the right of the 30 m location on the last plot sampled. For those stands with five trees sampled, we used the same methods but at fewer locations. The systematic sampling of trees ensured that their size and age were representative of the site. Within each density class the mean (\pm SE) DBH of trees sampled for radial growth (Table S2; low density= 5.3 ± 0.8 cm, med density = 3.1 ± 0.3 cm, high density = 2.7 ± 0.4 cm) was not significantly different from the mean DBH of all measured trees (Table 2; low density= 4.7 ± 0.4 cm, med density = 4.0 ± 0.4 cm, high density = 3.0 ± 0.4 cm) (t-value(t)=0.81 (low density), t-value(t)=0.81 (low density), t-value(t)=0.92 (high density);p-value>0.10).

Tree growth and stand productivity

All tree disks and cores were sanded with increasingly finer sandpaper (up to 400 grit) to produce visible rings. Annual ring widths were measured (resolution 0.001 mm) on each core and two radii per stem disk using WinDENDRO software version 2012c (Regent Instruments 2012). All subsequent sample preparation and analyses were completed using R statistical software version 3.6.0 (R Development Core Team 2018). We visually and statistically crossdated each tree-ring times series against master chronologies developed for each stand (Table S2) using the R package 'dplR' (Bunn 2010). Raw ring widths and individual tree measurements

of DBH were used to estimate annual basal area increment (BAI; mm² of wood year¹) for each core or radii using 'dplR' (Bunn 2010). Individual tree BAI chronologies were then built by averaging BAI of the two cores or radii measured for each tree (n=150). We chose to use BAI because it is a more direct measure of wood production than standardized tree ring width. BAI accounts for age and size related growth trends while maintaining both the high and low frequency variation in the tree ring time series (Biondi and Qeadan 2008) and is also a dependable metric for assessing long term growth trends (Peters et al. 2015). To ensure that we were not including juvenile growth in our analysis, all tree BAI chronologies were truncated at 1980 (Fig. 1).

To calculate stand BAI (m² ha⁻¹ year⁻¹) we averaged annual tree BAI (mm² year⁻¹) for each stand within each year, converted the average BAI to m² year⁻¹ and multiplied this by tree density (stems ha⁻¹) for each stand. Annual data on mortality and recruitment were not available over the 30-year tree ring record and thus could not be included in our metric of stand productivity. Supporting the exclusion of tree mortality and seedling recruitment in our metric of stand productivity, we saw little evidence of larch mortality or recruitment in our study sites. Furthermore, Alexander et al. (2012) used a chronosequence approach and found that both tree mortality and seedling recruitment were low in mid- to late succession larch forests across a range of tree densities in this region. Additionally, mid- to late successional forests have relatively thick organic soils that limit larch seedling recruitment and survival (Alexander et al. 2018). Our metric of stand productivity begins in 1980 when stands were approximately 40 years old and as such, both recruitment and mortality would be low to non-existent over this timeframe.

Climate data

We obtained monthly mean temperature (°C) and total precipitation (mm) from the Climate Research Unit high resolution time series data set (CRU TS 4.01 (Harris et al. 2013) for Cherskiy, Russia for the period 1980 to 2011 (Fig. 1). Data were extracted from the 0.5° x 0.5° grid cell containing the study sites. We calculated seasonal climate variables of mean temperature (°C) and total precipitation (mm) for fall (September, October, November), winter (December, January, February), spring (March, April, May), and growing season (June, July, August) (Fig. 1).

Normalized Difference Vegetation Index (NDVI) Data from Landsat

We estimated annual maximum summer NDVI from 1999 to 2011 for each site using 30-m resolution measurements of surface reflectance made by Landsat 5 and 7. The NDVI is derived from spectral reflectance in red and near-infrared wavelengths and ranges from -1 to 1 (Tucker 1979) with higher values typically associated with leafier, more productive vegetation (Pettorelli et al. 2005). The United States Geological Survey (USGS) recently generated the Landsat Collection 1 data set that includes Landsat 5 and 7 measurements corrected for atmospheric and terrain effects using the LEDAPS processing algorithm (Masek et al. 2006).

We used Google Earth Engine (Gorelick et al. 2017) to download all Landsat surface reflectance data that were acquired May through September from 1999 to 2011 for an approximate 90 x 90-m window centered on each site. Five stands (HDF1, MDF4, LBR, HDS1, and DAVY; Table S1) were located within 50 m of a dirt road that suppressed NDVI of some Landsat pixels in the window around these stands. To avoid the effect of the road, we systematically shifted these five stands 60 m to the south and west deeper into each stand prior to extracting the Landsat data. After extracting the data, we then excluded observations that were flagged as water, snow, cloud, or cloud shadow by the CFmask (Zhu and Woodcock 2014) and

215

216

217

218

219

220

221

222

223

224

225

226

227

228

229

230

231

232

233

234

235

236

additionally excluded observations from scenes with high solar zenith angle ($> 60^{\circ}$) or cloud cover (> 80%). Extensive filtering is necessary to identify clear-sky observations suitable for analysis of vegetation dynamics.

We estimated annual maximum NDVI for each stand using the clear-sky observations and a new phenology-based modeling approach (Berner et al. 2020). For each stand and Landsat scene, we computed mean surface reflectance of pixels within the 90 x 90-m window, derived NDVI using mean surface reflectance, and further cross-calibrated NDVI from Landsat 5 to Landsat 7 using published calibration coefficients (Ju and Masek 2016). We then estimated annual maximum NDVI using a new approach that helps alleviate issues with irregular timing of Landsat observations during the growing season, as well as the systematic underestimation of maximum NDVI if few scenes are available during a growing season (Berner et al. 2020). This approach involves (1) determining stand-specific land surface phenology during the growing season using flexible cubic splines fit through available NDVI data and (2) estimating annual maximum NDVI by adjusting individual growing season observations based on their likely phenological stage. To capture possible long-term changes in land surface phenology, a separate cubic spline is fit for each growing season using NDVI data from a multi-year window centered on that growing season (here \pm 3 years). To further guard against observations with poor data quality, the approach fits a cubic spline, removes observations that differ by >100% from the spline fit, and then repeats this process until there are no more outliers. The resulting phenological curves are then used with individual growing season observations to estimate annual maximum NDVI (Berner et al. 2020). A similar approach was previously used to evaluate interannual variation in the start and end of growing season using Landsat data across deciduous forests in parts of eastern North America (Melaas et al. 2013, 2016). We focused on the period

238

239

240

241

242

243

244

245

246

247

248

249

250

251

252

253

254

255

256

257

258

259

from 1999 to 2011 because Landsat data were not consistently acquired in this region until 1999 and the tree-ring data were available through 2011.

Statistical analysis

Annual trends in climate, growth, productivity, and NDVI

We examined trends for each of the eight seasonal climate parameters and for tree BAI (mm² year⁻¹) and stand BAI (m² ha⁻¹ year⁻¹) over the period of 1980-2011 and for NDVI over the period of 1999-2011 (Objective 1). To assess if and how seasonal climate parameters changed from 1980-2011 we fit simple linear regressions for each of the eight climate parameters as a function of year. Residuals for each model were checked for normality, homoscedasticity, and autocorrelation. To assess temporal changes in tree growth (tree BAI; mm² year⁻¹), stand productivity (stand BAI; m² ha⁻¹ year⁻¹), and NDVI we fit linear mixed effects models (LMM) using the package 'nlme' (Pinheiro et al. 2017). We natural log transformed tree BAI and stand BAI prior to analysis to meet the assumptions of normality. We modelled each of tree BAI, stand BAI, and NDVI with fixed effects of year, tree density category (low, medium, or high), and their interaction. For the response variable of tree BAI, we included random intercepts for stand and tree nested within stand to account for the spatial non-independence of trees within stands and the non-independence of annual BAI measurements within a tree. For the response variables of stand BAI and NDVI, we included stand as a random intercept. For each of these models, we tested if the inclusion of a random intercept of year and an autoregressive structure (AR1, autoregressive process of order one) improved model fits or changed model results (Appendix 1). In all cases, the inclusion of a random intercept for year and AR1 substantially increased the Akaike information criterion (AIC) indicating a reduced model fit (Zuur et al. 2009), but produced very similar results (Appendix 1). For these and all LMM that follow, we verified that

the statistical assumption of homogeneity of variance were not violated by visually inspecting residuals versus fitted values, all explanatory variables, and each grouping level of the random intercepts (Zuur et al. 2009). We also verified that our models accounted for the non-independence of measurements by examining autocorrelation plots of the residuals (Zuur et al. 2009). The significance of fixed effects were determined using maximum likelihood ratio tests (LRT) comparing the full model to a reduced model and confirmed using AIC (Δ AIC < 2.0) (Zuur et al. 2009). Optimal model coefficients were derived using restricted maximum likelihood estimation.

Impacts of density on stand structure, tree growth, stand productivity, and NDVI

To assess the effects of density on stand structure, tree growth, stand productivity, and NDVI (Objective 2), we first classified each stand into a tree density category (low, medium, or high). We tested for differences in stand averages of tree density, stand age, average tree diameter and basal area, canopy cover, active layer depth, soil organic layer depth, and C pools of larch trees, understory vegetation, and total aboveground vegetation between these categories using one-way analysis of variance (ANOVA). When differences were detected (p < 0.05), we completed Tukey adjusted pairwise comparisons between density categories.

To assess the effects of tree density on tree growth and stand productivity over the period 1980-2011 and NDVI over the period 1999-2011, we fit a LMM with a fixed effect of density category. For the response variables of tree BAI, we used random intercepts of stand and year nested within stand. For the response variables of site BAI and NDVI, we included a random intercept for year. We natural log transformed tree BAI and stand BAI prior to analysis. Model assumptions and the significance of fixed effects were assessed as described above. We tested

283

284

285

286

287

288

289

290

291

292

293

294

295

296

297

298

299

300

301

302

303

304

for differences in BAI and NDVI between each density class using a Tukey adjusted pairwise comparisons in the 'emmeans' package (Lenth et al. 2019).

Density dependent climate growth analyses

We assessed individual tree growth responses to climate over the period 1980-2011 (Objective 3) using two methods. We first calculated bootstrapped correlations between individual tree BAI and mean monthly temperatures and total monthly precipitation over a 17month climate window, extending from April of the year preceding growth to August of the current year of growth (Fritts 1976), using the package 'bootRes, version 1.2.3' (Zang 2010). The significance of each of the 34 climate correlations were determined from 95% confidence intervals (Zang 2010). These monthly correlations were done at the individual tree level in order to maintain the variation associated with each tree. Because we were interested in the effect of tree density on climate growth responses, we grouped trees based on tree density category (low, medium, high). The choice of detrending method can affect climate growth responses (Sullivan et al. 2016) and pre-whitening to remove autocorrelation is often done but is not recommended when using previous year climate variables (Zang and Biondi 2013). To assess the sensitivity of our results to detrending choice, we completed these bootstrapping analyses with raw ring width data, ring widths that were detrended using a modified negative exponential or the C-method, and prewhitened BAI chronologies (Appendix).

In addition to the descriptive monthly correlation analysis, we fit LMM to determine the effects of seasonal climate and tree density on productivity (Objective 3). This approach accounts for the temporal non-independence of measurements within individual trees and the spatial non-independence of trees located within stands and allows us to specifically test for the effects of tree density on growth responses to seasonal climate parameters. Seasonal climate

306

307

308

309

310

311

312

313

314

315

316

317

318

319

320

321

322

323

324

325

326

327

parameters were used instead of monthly due to collinearity of monthly variables. Based on variance inflation factors (VIF<3; Zuur et al. 2009) we did not detect multicollinearity between our seasonal climate parameters. We used natural log transformed individual tree BAI as the response variable and fixed effects of seasonal mean temperature, seasonal total precipitation, tree density category (low, medium, high), and the first order interaction between temperature or precipitation and tree density category. We scaled and centered all continuous climate predictor variables prior to model fitting. Since annual BAI represents repeated measures over the same individual trees located within stands, we included random intercepts for stand and tree nested within stand. Similar to the analysis described above, we also fit the model with AR1 and random intercepts of stand and year nested within stand. This increased the AIC but produced very similar results (Appendix 1). The significance of interaction terms were determined using maximum likelihood ratio tests comparing the full model to a reduced model without the interaction and confirmed using AIC (\triangle AIC < 2.0) (Zuur et al. 2009). For each of the seasonal climate parameters that significantly interacted with density class, we tested the significance of slopes for each density class and used a Tukey adjusted post hoc analysis for pairwise comparisons of slopes between density classes in the 'emmeans' package (Lenth et al. 2019). Similar to our bootstrapping analysis, we also completed these LMM using response variables derived from a variety of detrending methods and found that they all had similar results, supporting the robustness of our conclusions (Appendix 1).

NDVI and stand productivity analysis

To assess if annual changes in stand productivity were detected by NDVI at different tree densities (Objective 4), we first split the data into three tree density categories (low, medium, and high). For each category, we fit a LMM with a fixed effect of stand BAI and a random intercept

for stand. Model assumptions and the significance of fixed effects were assessed as described above.

Results

Fall, spring, and growing season temperatures increased over the period 1980-2011 (Objective 1; Table 1 and Fig. 1). Fall temperature increased the most, followed by spring and growing season temperatures. We found no significant trends in seasonal precipitation over the study period. In low density stands we found significant increases in tree growth and stand productivity, but in medium and high density stands both tree growth and stand productivity decreased from 1980-2011 (Objective 1; Table 1 and Table S3). NDVI increased at the same rate for all tree density categories from 1999-2011 (Objective 1; Table 1 and Table S3).

Average tree diameter (cm), tree basal area (m² ha¹), active layer depth (cm), and total understory C pools (Mg C ha¹) were greater in low density compared to high density stands. In contrast, canopy cover (%) and tree and total aboveground C pools (Mg C ha¹) were highest in high density stands and lowest in low density stands (Objective 2; Table 2). Tree growth (mm² yr¹) was significantly different between density categories, with two and a half times greater growth in low compared to high density stands (Objective 2; Table 2 and Table S4). Stand productivity (m² ha¹ yr¹) was also significantly different between density categories (Objective 2; Table 2 and Table S4). Productivity of high density stands was eight times greater than low density stands. Despite this greater productivity of high density stands, NDVI was highest in medium density stands and was not significantly different between low and high density stands (Objective 2; Table 2 and Table S4).

The response of tree growth to climate parameters varied with tree density. High and medium density stands generally responded negatively to temperature, whereas low density

stands responded positively to temperature (Objective 4; Fig. 3). Specifically, tree productivity in low density stands was positively correlated to previous fall (September through November) and current summer (June, July, August) temperatures, whereas tree productivity in high and medium density stands was negatively correlated to previous spring and summer (April through July) temperatures. Correlations to precipitation were more variable than correlations to temperature in low density stands, but growth generally increased with higher previous fall precipitation (Fig. 3). Growth of trees in high and medium density stands was positively correlated to precipitation in July of the previous year.

We observed similar growth responses to climate using a mixed-model approach. The effects of climate on growth differed between density categories for most climate parameters, but not for winter and current growing season temperatures (Objective 4; Table 3 and Table S5 and Table S6). In general, high and medium density stands exhibited negative growth responses to temperature, whereas low density stands exhibited positive growth responses to temperature, with previous fall temperature exhibiting the strongest positive effect on growth (Table 3). Similar to the bootstrapping results, effects of precipitation were more variable. We observed both negative and positive effects of precipitation on productivity in low density stands and positive or neutral effects on growth in high and medium density stands.

NDVI captured annual variation in stand productivity (m² ha⁻¹ yr⁻¹) in all stand density categories (Objective 5; Fig. 3 and Table S7).

Discussion

As climate continues to warm, the northern extent of the boreal forest is expect to shift northward, leading to increased tree density throughout the present TTE (Holtmeier and Broll 2007; Larsen et al. 2014). In this study, we examined stands that established following a 1940

fire in Northeast Siberia and represent a large range in Cajander larch tree densities. We assessed the potential impacts of increased tree density on tree growth responses to climate and determined if patterns of stand productivity are captured by NDVI. We found that high density stands with shallow active layers had lower individual tree growth and more negative growth responses to growing season temperatures compared to low density stands with deep active layers. This suggests that increased tree density in the TTE can lead to increased competition for moisture and suppress the ability of trees to increase growth in response to climate warming.

NDVI was able to capture annual variability in stand productivity within stand density categories but did not capture differences in productivity associated with changes in tree density.

In low density stands, we observed increases of both individual tree growth and stand productivity from 1980-2011, whereas both growth and productivity in medium and high density stands decreased. These density dependent trends suggest that competition for resources is limiting the ability of trees to respond positively to the increases in temperature we observed in this region. However, declines in larch productivity have also been observed in older (98 -234 years) low to medium density stands in the same region since the 1940s (Berner et al. 2013), suggesting that the increase in productivity we observed in younger (~75 years) low density stands might not continue as stands mature.

Tree growth is often suppressed in higher density stands compared to lower density stands due to increased competition for water, nutrients, and light (Fritts 1976). However, when scaled to overall stand productivity, increased density can more than compensate for the reduced growth of individual trees. This compensatory response is well established and commonly used in forest growth yield models (Assmann 1970), but these dynamics have not been assessed at the latitudinal limit of the boreal forest where stand densities have historically been low but are now

increasing (Kharuk et al. 2013b; Lantz et al. 2019). In fact, only the low density stands (300 to 3500 stems ha⁻¹) had canopy covers (<20%) consistent with the delineation of the TTE (Ranson et al. 2011) despite the high latitude (~68.74° N) of all study sites. Our findings support this compensatory response with tree growth being lowest and overall stand productivity being highest in high density stands compared to medium or low density stands. High density stands also had significantly thinner active layers, indicating lower soil volume for water and nutrient uptake (Kropp et al. 2019), which can reduce tree growth (Kirdyanov et al. 2020). A shallow active layer and canopy shading in high density stands also corresponds to lower soil temperatures (Kropp et al. 2019), which could limit soil organic matter decomposition and the availability of nitrogen and other nutrients required for boreal tree growth (Tamm 1991). However, there is no evidence of increased density resulting in lower nitrogen supply or greater intraspecific competition for nitrogen in these forest stands (Hewitt et al. in prep). Taken together, these results suggest that competitive interactions for water or light might be limiting individual tree growth in high density stands.

We observed the effects of competitive interactions on the ability of trees to respond positively to increasing temperatures. The climate-growth responses of larch trees in high and medium density stands differed from those in low density stands and from previous research in this region (Berner et al. 2013). In low density stands, we saw a positive effect of previous fall temperature on tree growth which has also been observed in larch forests of North America (Girardin et al. 2005). These growth responses suggest that a lengthening of the growing season delays leaf senescence and increases photosynthetic activity, allowing trees to store more carbohydrates for the subsequent growing season. An earlier spring snowmelt via increased spring temperatures and reduced spring precipitation that falls as snow can also increase the

421

422

423

424

425

426

427

428

429

430

431

432

433

434

435

436

437

438

439

440

441

442

growing season length. Although earlier snowmelt can reduce growth (Girardin et al. 2005), it can also enhance wood production in the growing season due to an earlier onset of xylogenesis (Kirdyanov et al. 2003). This explains the positive effect of current spring temperature and negative effect of current spring precipitation on growth in low density stands. Our results concur with previous work that showed positive growth response to early summer temperature in low to moderately dense larch stands over the period 1938 to 2007 in this region (Berner et al. (2013), while also highlighting that growth response to early summer temperatures is strongly affected by tree density.

The tree growth responses to climate that we observed in high and medium density stands are consistent with a drought stress response that has been reported for larch and pine trees in central and southern Siberia (Sidorova et al. 2009; Kharuk et al. 2013a) and black spruce (Picea mariana) and white spruce (*Picea glauca*) throughout Alaska (Wilmking et al. 2004; Walker and Johnstone 2014). Our results also support conclusions based on larch transpiration and stomatal conductance (Kropp et al. 2019) that productivity in high density stands with a shallow active layer might be limited by water availability. Negative responses of productivity to previous spring and growing season temperatures, positive responses to both previous and current spring and growing season precipitation, and positive responses to winter precipitation are indicative of drought stress. Drought stress in these high density stands can occur through: (i) increased competition for soil water (Wilmking et al. 2004); (ii) low snow depths during the winter delaying spring soil thaw, which if combined with warm temperatures result in insufficient water transport from roots to support evaporative demands (Berg and Chapin III 1994); and (iii) low albedo and high thermal absorption increasing leaf temperatures and transpiration rates and suspending photosynthesis (Brooks et al. 1998). A shallow active layer that limits the rooting

444

445

446

447

448

449

450

451

452

453

454

455

456

457

458

459

460

461

462

463

464

465

depth of trees and makes them less effective at water uptake has also been proposed as a drought stress mechanism (Walker and Johnstone 2014). However, larch rooting depth did not differ between tree density categories and was primarily constrained to the organic layer (Kropp et al., 2019), the depth of which did not differ between tree densities (Table 2). Although we cannot definitively conclude the mechanism for this drought stress response, we expect that if air temperatures continuing increasing without an increase in precipitation, the productivity of trees in high density stands with a thin active layer could become progressively limited by water availability.

We found that Landsat NDVI did not differ between low and high density stands despite an approximate eight-fold difference in stand-level tree productivity. The NDVI scales near linearly with the fraction of incident photosynthetically active radiation (PAR) absorbed by the land surface (Myneni and Williams 1994), which is a key determinant of total absorbed PAR and subsequent primary productivity (Goetz and Prince 1999; Glenn et al. 2008). We suspect the similarity in NDVI irrespective of tree density or productivity arose because Landsat NDVI integrates contributions from both overstory and understory vegetation, whereas the field measurements captured only the overstory component of primary productivity. Our results suggest that understory vegetation productivity exerts strong influence on remotely-sensed NDVI in areas with low tree density, potentially compensating for lower tree productivity. These results are consistent with there being little correlation ($r \approx 0.33$) between Landsat NDVI and larch aboveground biomass in this region (Berner et al. 2012), as well as with the observation that understory NDVI can exceed overstory NDVI in larch stands due to canopy structure and shadows (Loranty et al. 2018). Overall, these findings highlight that remotely-sensed NDVI may not detect expected warming-induced increases in tree density in the TTE.

467

468

469

470

471

472

473

474

475

476

477

478

479

480

481

482

483

484

485

486

487

488

Our analysis showed that Landsat NDVI detected inter-annual variability in stand-level tree productivity regardless of tree density. Prior studies have report a positive relationship between coarse resolution AVHRR (~8 km) and MODIS (~1 km) NDVI and tree ring width at sites around the globe (Vicente-Serrano et al. 2016). However, the strength of relationship has varied from not significant or very weak at treeline sites in North America (Beck et al. 2013; Brehaut and Danby 2018) to moderate and strong at some sites in Russia, Interior Alaska, and the Northwest Territories (Beck et al. 2011; Berner et al. 2011; Bunn et al. 2013). We observed a positive relationship between inter-annual variability in Landsat NDVI and stand-level tree productivity across the density gradient stands. These results corroborate with previous research showing that forest cover (%) had no impact on the relationship between NDVI and ring width in northwestern Canada or northeastern Russia (Berner et al. 2011; Brehaut and Danby 2018). Whether in the TTE or elsewhere, it is currently unclear if moderate resolution Landsat NDVI better tracks stand-level tree growth than far coarser resolution AVHRR and MODIS NDVI. Landsat NDVI time series are increasingly being used to infer forest and tundra response to climate change at northern high latitudes (e.g. Ju and Masek 2016; Sulla-Menashe et al. 2018; Berner et al. 2020). Future efforts should therefore focus on evaluating links between Landsat NDVI and field measurements of plant productivity and other biophysical characteristics in the TTE and surrounding regions.

A potential limitation of our study is that we only sampled 5 to 10 trees per stand. These trees were randomly sampled and representative of tree size within the stand but could fail to capture important individual tree growth dynamics. Scaling to the stand level based on a relatively low sample size could exacerbate the effects of these potentially missing growth dynamics. We were also unable to include recruitment or mortality in our metric of stand

productivity over the 30-year tree ring record. A single post-fire cohort dominates these stands and Cajander larch trees are relatively long-lived (Alexander et al. 2012). Therefore, both mortality and recruitment are low to non-existent and so their contribution to stand productivity would be unlikely to affect our results or conclusions. The short period of overlapping tree-ring and satellite data (13 years) also constrains interpretation of our results linking productivity to NDVI. Despite these potential limitations, our data and analyses still provide valuable insights into the impacts of tree density on tree growth responses to climate and the ability of NDVI to capture annual variation in stand productivity.

Conclusions

In this study, we show that increases in tree density can suppress the positive response of individual tree growth to climate warming, but results in an overall higher stand productivity. Landsat NDVI did not detect this higher stand productivity. The expected increase in tree density in the TTE is therefore unlikely to be captured by NDVI in this region. We emphasize that increased density and a shallow active layer in the TTE have the potential to enhance competitive interactions and result in growth reductions and temperature induced drought stress with continued climate warming. Landsat NDVI has the potential to capture these interannual variations in stand productivity within density categories. We conclude that there is a need to incorporate changes in tree density and the resulting density dependent responses of trees to climate into models and predictions of changes at the northern limit of the boreal forest.

509

Acknowledgments

- This project was supported by funding from the National Science Foundation's (NSF) Division
- of Polar Programs to MCM (PLR 1545558 and PLR 1708344) and HDA (PLR 1304040 and
- 511 PLR 1708307) and from NSF Arctic Natural Sciences to Scott Goetz (16-61723).

References

- Alexander, H.D., Mack, M.C., Goetz, S., Loranty, M.M., Beck, P.S., Earl, K., Zimov, S., Davydov, S., and Thompson, C.C. 2012. Carbon accumulation patterns during post-fire succession in Cajander larch (Larix cajanderi) forests of Siberia. Ecosystems **15**(7): 1065–1082.
 - Alexander, H.D., Natali, S.M., Loranty, M.M., Ludwig, S.M., Spektor, V.V., Davydov, S., Zimov, N., Trujillo, I., and Mack, M.C. 2018. Impacts of increased soil burn severity on larch forest regeneration on permafrost soils of far northeastern Siberia. Forest Ecology and Management 417: 144–153. doi:10.1016/j.foreco.2018.03.008.
 - Arctic Monitoring and Assessment Programme. 2017. Snow, Water, Ice and Permafrost in the Arctic (SWIPA). Available from https://www.amap.no/documents/doc/snow-water-ice-and-permafrost-in-the-arctic-swipa-2017/1610 [accessed 17 July 2019].
 - Assmann, E. (*Editor*). 1970. Copyright. *In* The Principles of Forest Yield Study. Pergamon. p. iv. doi:10.1016/B978-0-08-006658-5.50002-9.
 - Beck, P.S.A., Andreu-Hayles, L., D'Arrigo, R., Anchukaitis, K.J., Tucker, C.J., Pinzón, J.E., and Goetz, S.J. 2013. A large-scale coherent signal of canopy status in maximum latewood density of tree rings at arctic treeline in North America. Global and Planetary Change **100**: 109–118. doi:10.1016/j.gloplacha.2012.10.005.
 - Beck, P.S.A., and Goetz, S.J. 2011. Satellite observations of high northern latitude vegetation productivity changes between 1982 and 2008: ecological variability and regional differences. Environmental Research Letters **6**(4): 045501.
 - Beck, P.S.A., Juday, G.P., Alix, C., Barber, V.A., Winslow, S.E., Sousa, E.E., Heiser, P., Herriges, J.D., and Goetz, S.J. 2011. Changes in forest productivity across Alaska consistent with biome shift. Ecology Letters **14**(4): 373–379. doi:10.1111/j.1461-0248.2011.01598.x.
 - Berg, E.E., and Chapin III, F.S. 1994. Needle loss as a mechanism of winter drought avoidance in boreal conifers. Canadian Journal of Forest Research **24**(6): 1144–1148. doi:10.1139/x94-151.
 - Berner, L.T., Beck, P.S.A., Bunn, A.G., and Goetz, S.J. 2013. Plant response to climate change along the forest-tundra ecotone in northeastern Siberia. Global Change Biology **19**(11): 3449–3462. doi:10.1111/gcb.12304.
 - Berner, L.T., Beck, P.S.A., Bunn, A.G., Lloyd, A.H., and Goetz, S.J. 2011. High-latitude tree growth and satellite vegetation indices: Correlations and trends in Russia and Canada (1982–2008). Journal of Geophysical Research 116(G1). doi:10.1029/2010JG001475.
 - Berner, L.T., Beck, P.S.A., Loranty, M.M., Alexander, H.D., Mack, M.C., and Goetz, S.J. 2012. Cajander larch (Larix cajanderi) biomass distribution, fire regime and post-fire recovery in northeastern Siberia. Biogeosciences **9**(10): 3943–3959.
 - Berner, L.T., Massey, R., Jantz, P., Forbes, B.C., Macias-Fauria, M., Myers-Smith, I., Kumpula, T., Gauthier, G., Andreu-Hayles, L., Gaglioti, B.V., Burns, P., Zetterberg, P., D'Arrigo, R., and Goetz, S.J. 2020. Summer warming explains widespread but not uniform greening in the Arctic tundra biome. Nature Communications 11(1): 1–12. Nature Publishing Group. doi:10.1038/s41467-020-18479-5.
 - Biondi, F., and Qeadan, F. 2008. A theory-driven approach to tree-ring standardization: defining the biological trend from expected basal area increment. Tree-Ring Research **64**(2): 81–96.
 - Brehaut, L., and Danby, R.K. 2018. Inconsistent relationships between annual tree ring-widths and satellite-measured NDVI in a mountainous subarctic environment. Ecological Indicators **91**: 698–711. doi:10.1016/j.ecolind.2018.04.052.
 - Brooks, J.R., Flanagan, L.B., and Ehleringer, J.R. 1998. Responses of boreal conifers to climate fluctuations: indications from tree-ring widths and carbon isotope analyses. Canadian Journal of Forest Research-Revue Canadienne De Recherche Forestiere **28**(4): 524–533.
 - Brown, C.D. 2010. Tree-line Dynamics: Adding Fire to Climate Change Prediction. Arctic **63**(4): 488–492.

- Bunn, A.G. 2010. Statistical and visual crossdating in R using the dplR library. Dendrochronologia **28**(4): 251–258. doi:10.1016/j.dendro.2009.12.001.
 - Bunn, A.G., Hughes, M.K., Kirdyanov, A.V., Losleben, M., Shishov, V.V., Berner, L.T., Oltchev, A., and Vaganov, E.A. 2013. Comparing forest measurements from tree rings and a space-based index of vegetation activity in Siberia. Environ. Res. Lett. **8**(3): 035034. doi:10.1088/1748-9326/8/3/035034.
 - Callaghan, T.V., Crawford, R.M.M., Eronen, M., Hofgaard, A., Payette, S., Rees, W.G., Skre, O., Sveinbjörnsson, B., Vlassova, T.K., and Werkman, B.R. 2002. The dynamics of the tundra-taiga boundary: An overview and suggested coordinated and integrated approach to research. Ambio 31: 3–5.
 - Fritts, H.C. 1976. Tree Rings and Climate. Academic Press, London.
 - Gea-Izquierdo, G., Martin-Benito, D., Cherubini, P., and Canellas, I. 2009. Climate-growth variability in Quercus ilex L. west Iberian open woodlands of different stand density. Annals of Forest Science **66**(8). doi:10.1051/forest/2009080.
 - Girardin, M.-P., Berglund, E., Tardif, J.C., and Monson, K. 2005. Radial Growth of Tamarack (Larix laricina) in the Churchill Area, Manitoba, Canada, in Relation to Climate and Larch Sawfly (Pristiphora erichsonii) Herbivory. Arctic, Antarctic, and Alpine Research 37(2): 206–217. doi:10.1657/1523-0430(2005)037[0206:RGOTLL]2.0.CO;2.
 - Glenn, E.P., Huete, A.R., Nagler, P.L., and Nelson, S.G. 2008. Relationship Between Remotely-sensed Vegetation Indices, Canopy Attributes and Plant Physiological Processes: What Vegetation Indices Can and Cannot Tell Us About the Landscape. Sensors (Basel) 8(4): 2136–2160. doi:10.3390/s8042136.
 - Goetz, S.J., and Prince, S.D. 1999. Modelling Terrestrial Carbon Exchange and Storage: Evidence and Implications of Functional Convergence in Light-use Efficiency. *In* Advances in Ecological Research. *Edited by* A.H. Fitter and D. Raffaelli. Academic Press. pp. 57–92. doi:10.1016/S0065-2504(08)60029-X.
 - Gomez-Aparicio, L., Garcia-Valdes, R., Ruiz-Benito, P., and Zavala, M.A. 2011. Disentangling the relative importance of climate, size and competition on tree growth in Iberian forests: implications for forest management under global change. Global Change Biology **17**(7): 2400–2414.
 - Gorelick, N., Hancher, M., Dixon, M., Ilyushchenko, S., Thau, D., and Moore, R. 2017. Google Earth Engine: Planetary-scale geospatial analysis for everyone. Remote Sensing of Environment **202**: 18–27. doi:10.1016/j.rse.2017.06.031.
 - Harris, I., Jones, P., Osborn, T., and Lister, D. 2013. Updated high-resolution grids of monthly climatic observations—the CRU TS3. 10 Dataset. International Journal of Climatology.
 - Harsch, M.A., Hulme, P.E., McGlone, M.S., and Duncan, R.P. 2009. Are treelines advancing? A global meta-analysis of treeline response to climate warming. Ecology Letters **12**(10): 1040–1049.
 - Hewitt, R.E., Alexander, H.A., Izbicki, B., Loranty, M.A., Natali, S.M., Walker, X.J., Mack. M.C. Scale-dependent effects of tree density on aboveground and belowground nitrogen cycling at the taigatundra ecotone. *In prep*
 - Holtmeier, F.K., and Broll, G. 2007. Treeline advance driving processes and adverse factors. Landscape Online 1: 1–33.
 - Ju, J., and Masek, J.G. 2016. The vegetation greenness trend in Canada and US Alaska from 1984–2012 Landsat data. Remote Sensing of Environment 176: 1–16. Elsevier.
 - Kharuk, V.I., Im, S.T., Oskorbin, P.A., Petrov, I.A., and Ranson, K.J. 2013a. Siberian pine decline and mortality in southern siberian mountains. Forest Ecology and Management 310: 312–320. doi:10.1016/j.foreco.2013.08.042.
 - Kharuk, V.I., Ranson, K.J., Im, S.T., Oskorbin, P.A., Dvinskaya, M.L., and Ovchinnikov, D.V. 2013b. Tree-Line Structure and Dynamics at the Northern Limit of the Larch Forest: Anabar Plateau, Siberia, Russia. Arctic, Antarctic, and Alpine Research **45**(4): 526–537. Taylor & Francis. doi:10.1657/1938-4246-45.4.526.

- Kirdyanov, A., Hughes, M., Vaganov, E., Schweingruber, F., and Silkin, P. 2003. The importance of early summer temperature and date of snow melt for tree growth in the Siberian Subarctic. Trees 17(1): 61–69. doi:10.1007/s00468-002-0209-z.
 - Kirdyanov, A.V., Saurer, M., Siegwolf, R., Knorre, A.A., Prokushkin, A.S., Churakova (Sidorova), O.V., Fonti, M.V., and Büntgen, U. 2020. Long-term ecological consequences of forest fires in the continuous permafrost zone of Siberia. Environmental Research Letters **15**(3): 034061. doi:10.1088/1748-9326/ab7469.
 - van der Kolk, H.-J., Heijmans, M.M., van Huissteden, J., Pullens, J.W., and Berendse, F. 2016. Potential Arctic tundra vegetation shifts in response to changing temperature, precipitation and permafrost thaw. Biogeosciences 13: 6229–6245. Copernicus Publications on behalf of the European Geosciences Union.
 - Kropp, H., Loranty, M.M., Natali, S.M., Kholodov, A.L., Alexander, H.D., Zimov, N.S., Mack, M.C., and Spawn, S.A. 2019. Tree density influences ecohydrological drivers of plant–water relations in a larch boreal forest in Siberia. Ecohydrology **0**(0): e2132. doi:10.1002/eco.2132.
 - Landhausser, S.M., and Wein, R.W. 1993. Postfire vegetation recovery and tree establishment at the Arctic treeline: climate-change/vegetation-response hypotheses. Journal of Ecology **81**(4): 665–672.
 - Lantz, T.C., Moffat, N.D., Fraser, R.H., and Walker, X. 2019. Reproductive limitation mediates the response of white spruce (Picea glauca) to climate warming across the forest–tundra ecotone. Arctic Science 5(4): 167–184. NRC Research Press. doi:10.1139/as-2018-0012.
 - Larsen, J.N., Anisimov, O.A., Constable, A., Hollowed, A.B., Maynard, N., and Prestrud, P. 2014. Polar regions In: Barros VR, Field CB, Dokken DJ, Mastrandrea MD, Mach KJ, Bilir TE, et al., editors. Climate Change 2014: Impacts, Adaptation, and Vulnerability Part B: Regional Aspects Contribution of Working Group II to the Fifth Assessment Report of the Intergovernmental Panel on Climate Change. New York: Cambridge University Press.
 - Lenoir, J., and Svenning, J.-C. 2015. Climate-related range shifts a global multidimensional synthesis and new research directions. Ecography **38**(1): 15–28. doi:10.1111/ecog.00967.
 - Lenth, R., Singmann, H., Love, J., Buerkner, P., and Herve, M. 2019. emmeans: Estimated Marginal Means, aka Least-Squares Means. Available from https://CRAN.R-project.org/package=emmeans [accessed 18 April 2019].
 - Liang, E., Wang, Y., Piao, S., Lu, X., Camarero, J.J., Zhu, H., Zhu, L., Ellison, A.M., Ciais, P., and Peñuelas, J. 2016. Species interactions slow warming-induced upward shifts of treelines on the Tibetan Plateau. Proc Natl Acad Sci U S A 113(16): 4380–4385. doi:10.1073/pnas.1520582113.
 - Linares, J.C., Camarero, J.J., and Carreira, J.A. 2010. Competition modulates the adaptation capacity of forests to climatic stress: insights from recent growth decline and death in relict stands of the Mediterranean fir Abies pinsapo. Journal of Ecology **98**(3): 592–603.
 - Loranty, M.M., Davydov, S.P., Kropp, H., Alexander, H.D., Mack, M.C., Natali, S.M., and Zimov, N.S. 2018. Vegetation indices do not capture forest cover variation in upland Siberian larch forests. Remote Sensing **10**(11): 1686. doi:10.3390/rs10111686.
 - Masek, J.G., Vermote, E.F., Saleous, N.E., Wolfe, R., Hall, F.G., Huemmrich, K.F., Gao, F., Kutler, J., and Lim, T.-K. 2006. A Landsat Surface Reflectance Dataset for North America, 1990–2000. IEEE Geoscience and Remote Sensing Letters **3**(1): 68–72. doi:10.1109/LGRS.2005.857030.
 - Melaas, E.K., Friedl, M.A., and Zhu, Z. 2013. Detecting interannual variation in deciduous broadleaf forest phenology using Landsat TM/ETM+ data. Remote Sensing of Environment **132**: 176–185. doi:10.1016/j.rse.2013.01.011.
 - Melaas, E.K., Sulla-Menashe, D., Gray, J.M., Black, T.A., Morin, T.H., Richardson, A.D., and Friedl, M.A. 2016. Multisite analysis of land surface phenology in North American temperate and boreal deciduous forests from Landsat. Remote Sensing of Environment 186: 452–464. doi:10.1016/j.rse.2016.09.014.

- Montesano, P.M., Neigh, C., Macander, M.J., Feng, M., and Noojipady, P. 2020. The bioclimatic extent
 and pattern of the cold edge of the boreal forest: the circumpolar taiga-tundra ecotone. Environ.
 Res. Lett. IOP Publishing. doi:10.1088/1748-9326/abb2c7.
 - Myers-Smith, I.H., Kerby, J.T., Phoenix, G.K., Bjerke, J.W., Epstein, H.E., Assmann, J.J., John, C., Andreu-Hayles, L., Angers-Blondin, S., and Beck, P.S. 2020. Complexity revealed in the greening of the Arctic. Nature Climate Change **10**(2): 106–117. Nature Publishing Group.
 - Myneni, R.B., and Williams, D.L. 1994. On the relationship between FAPAR and NDVI. Remote Sensing of Environment **49**(3): 200–211. doi:10.1016/0034-4257(94)90016-7.
 - Nemani, R.R., Keeling, C.D., Hashimoto, H., Jolly, W.M., Piper, S.C., Tucker, C.J., Myneni, R.B., and Running, S.W. 2003. Climate-driven increases in global terrestrial net primary production from 1982 to 1999. Science **300**(5625): 1560–1563.
 - Paulson, A.K., Peña III, H., Alexander, H.D., Davydov, S.P., Loranty, M.M., Mack, M.C., Natali, S.M. *In press*. Understory plant diversity and composition across a post-fire tree density gradient in a Siberian Arctic boreal forest. *Canadian Journal of Forest Research*. 10.1139/cjfr-2020-0483
 - Pearson, R.G., Phillips, S.J., Loranty, M.M., Beck, P.S.A., Damoulas, T., Knight, S.J., and Goetz, S.J. 2013. Shifts in Arctic vegetation and associated feedbacks under climate change. Nature Climate Change 3(7): 673–677. doi:10.1038/nclimate1858.
 - Peters, R.L., Groenendijk, P., Vlam, M., and Zuidema, P.A. 2015. Detecting long-term growth trends using tree rings: a critical evaluation of methods. Global Change Biology **21**(5): 2040–2054. doi:10.1111/gcb.12826.
 - Pettorelli, N., Vik, J.O., Mysterud, A., Gaillard, J.-M., Tucker, C.J., and Stenseth, N.Chr. 2005. Using the satellite-derived NDVI to assess ecological responses to environmental change. Trends in Ecology & Evolution **20**(9): 503–510. doi:10.1016/j.tree.2005.05.011.
 - Pinheiro, J., Bates, D., DebRoy, S., Sarkar, D., Heisterkamp, S., Van Willigen, B., and Maintainer, R. 2017. Package 'nlme.' Linear and Nonlinear Mixed Effects Models, version: 3–1.
 - R Development Core Team. 2018. R: A language and environment for statistical computing.
 - Ranson, K.J., Montesano, P.M., and Nelson, R. 2011. Object-based mapping of the circumpolar taigatundra ecotone with MODIS tree cover. Remote Sensing of Environment **115**(12): 3670–3680. doi:10.1016/j.rse.2011.09.006.
 - Rees, W.G., Hofgaard, A., Boudreau, S., Cairns, D.M., Harper, K., Mamet, S., Mathisen, I., Swirad, Z., and Tutubalina, O. 2020. Is subarctic forest advance able to keep pace with climate change? Global Change Biology. John Wiley & Sons, Ltd. doi:10.1111/gcb.15113.
 - Rickbeil, G.J.M., Hermosilla, T., Coops, N.C., White, J.C., Wulder, M.A., and Lantz, T.C. 2018. Changing northern vegetation conditions are influencing barren ground caribou (Rangifer tarandus groenlandicus) post-calving movement rates. Journal of Biogeography **45**(3): 702–712. doi:10.1111/jbi.13161.
 - Sidorova, O.V., Siegwolf, R.T.W., Saurer, M., Shashkin, A.V., Knorre, A.A., Prokushkin, A.S., Vaganov, E.A., and Kirdyanov, A.V. 2009. Do centennial tree-ring and stable isotope trends of Larix gmelinii (Rupr.) Rupr. indicate increasing water shortage in the Siberian north? Oecologia **161**(4): 825–835. doi:10.1007/s00442-009-1411-0.
 - Sulla-Menashe, D., Woodcock, C.E., and Friedl, M.A. 2018. Canadian boreal forest greening and browning trends: an analysis of biogeographic patterns and the relative roles of disturbance versus climate drivers. Environ. Res. Lett. **13**(1): 014007. IOP Publishing. doi:10.1088/1748-9326/aa9b88.
 - Sullivan, P.F., Pattison, R.R., Brownlee, A.H., Cahoon, S.M.P., and Hollingsworth, T.N. 2016. Effect of tree-ring detrending method on apparent growth trends of black and white spruce in interior Alaska. Environ. Res. Lett. **11**(11): 114007. IOP Publishing. doi:10.1088/1748-9326/11/11/114007.
 - Tamm, C.O. 1991. Nitrogen in Terrestrial Ecosystems: Questions of Productivity, Vegetational Changes, and Ecosystem Stability. Springer-Verlag, Berlin Heidelberg. Available from https://www.springer.com/gp/book/9783642751707 [accessed 2 October 2019].

- Veraverbeke, S., Rogers, B.M., Goulden, M.L., Jandt, R.R., Miller, C.E., Wiggins, E.B., and Randerson, J.T. 2017. Lightning as a major driver of recent large fire years in North American boreal forests. Nature Climate Change 7(7): 529–534. doi:10.1038/nclimate3329.
- Vicente-Serrano, S.M., Camarero, J.J., Olano, J.M., Martín-Hernández, N., Peña-Gallardo, M., Tomás-Burguera, M., Gazol, A., Azorin-Molina, C., Bhuyan, U., and El Kenawy, A. 2016. Diverse relationships between forest growth and the Normalized Difference Vegetation Index at a global scale. Remote Sensing of Environment **187**: 14–29. doi:10.1016/j.rse.2016.10.001.
- Walker, X., and Johnstone, J.F. 2014. Widespread negative correlations between black spruce growth and temperature across topographic moisture gradients in the boreal forest. Environmental Research Letters **9**(6): 064016.
- Wang, Y., Pederson, N., Ellison, A.M., Buckley, H.L., Case, B.S., Liang, E., and Camarero, J.J. 2016. Increased stem density and competition may diminish the positive effects of warming at alpine treeline. Ecology **97**(7): 1668–1679. doi:10.1890/15-1264.1.
- Wilmking, M., Juday, G.P., Barber, V.A., and Zald, H.S.J. 2004. Recent climate warming forces contrasting growth responses of white spruce at treeline in Alaska through temperature thresholds. Global Change Biology **10**(10): 1724–1736. doi:10.1111/j.1365-2486.2004.00826.x.
- de Wit, H.A., Bryn, A., Hofgaard, A., Karstensen, J., Kvalevåg, M.M., and Peters, G.P. 2014. Climate warming feedback from mountain birch forest expansion: reduced albedo dominates carbon uptake. Global Change Biology **20**(7): 2344–2355. Wiley Online Library.
- Zang, C. 2010. bootRes: Bootstrapped response and correlation functions. R package version 0.3. http://cran.r-project.org/web/packages/bootRes/.
- Zang, C., and Biondi, F. 2013. Dendroclimatic calibration in R: The bootRes package for response and correlation function analysis. Dendrochronologia 31(1): 68–74. doi:10.1016/j.dendro.2012.08.001.
- Zhang, W., Miller, P.A., Smith, B., Wania, R., Koenigk, T., and Döscher, R. 2013. Tundra shrubification and tree-line advance amplify arctic climate warming: results from an individual-based dynamic vegetation model. Environ. Res. Lett. 8(3): 034023. doi:10.1088/1748-9326/8/3/034023.
- Zhu, Z., and Woodcock, C.E. 2014. Continuous change detection and classification of land cover using all available Landsat data. Remote sensing of Environment **144**: 152–171. Elsevier.
- Zuur, A., Ieno, E.N., Walker, N., Saveliev, A.A., and Smith, G.M. 2009. Mixed effects models and extensions in ecology with R. Springer Science & Business Media.

Table Legends

Table 1. Trends in climate, tree growth, stand productivity, and NDVI over time. Values represent the annual estimated change in the response variable over the period 1980 to 2011, except for NDVI which covers the period from 1999 to 2011. Tree growth and stand productivity were natural log transformed prior to analysis but effect sizes are on the original scale. For tree growth and stand productivity (mixed model results in Table S3) superscript letters represent significant (P<0.05) differences between the slopes of the three density categories as determined by Tukey post-hoc pairwise comparisons. For NDVI, there was no interaction between year and NDVI, thus only one value is presented (Table S3). For all models, red text indicates a negative trend, black indicates a positive trend, and shaded cells represent a significant effect. See Fig. 1 for raw data plotted over time.

Table 2. Average (± standard error) variables summarized by density category. Bolded variables were significantly different (P<0.05) among density categories. Superscript letters represent differences between categories. See Table S4 for linear mixed effects model results of the effect of density category on tree growth, stand productivity, and NDVI.

Table 3. Marginal mean estimates of the effect of seasonal climate variables on tree growth (basal area increment; mm^2 year⁻¹). Letters represent significant differences between density categories based on Tukey adjusted post-hoc pairwise comparisons (P<0.05). Note that model was fit on centered and scaled predictor variables and a natural log transformed response variable, but the estimated effect sizes presented here are on the original scale. Shaded cells represent a significant slope (P <0.05); red indicates a negative effect and grey indicates a positive effect. See Table S5 for the full model and Table S6 for reduced model results (marginal R^2 =0.16; conditional R^2 =0.83).

Table 1. Trends in climate, tree growth, stand productivity, and NDVI over time. Values represent the annual estimated change in the response variable over the period 1980 to 2011, except for NDVI which covers the period from 1999 to 2011. Tree growth and stand productivity were natural log transformed prior to analysis but effect sizes are on the original scale. For tree growth and stand productivity (mixed model results in Table S3) superscript letters represent significant (P<0.05) differences between the slopes of the three density categories as determined by Tukey post-hoc pairwise comparisons. For NDVI, there was no interaction between year and NDVI, thus only one value is presented (Table S3). For all models, red text indicates a negative trend, black indicates a positive trend, and shaded cells represent a significant effect. See Fig. 1 for raw data plotted over time.

Mode	el	Effect ± st.error	t-value	\mathbb{R}^2	p-value
• •	Fall	0.11 ± 0.03	4.67	0.38	< 0.001
Temperature	Winter	-0.01 ± 0.03	-0.66	0	0.52
npei	Spring	0.10 ± 0.02	3.49	0.25	< 0.01
Te	Growing Season	0.06 ± 0.02	3.68	0.28	< 0.001
	Fall	0.24 ± 0.25	0.97	0	0.34
tatio	Winter	-0.24 ± 0.14	-1.63	0.05	0.11
Precipitation	Spring	0.01 ± 0.09	0.18	-0.03	0.86
Pre	Growing Season	0.09 ± 0.38	0.25	-0.03	0.80
	Low	2.76 ± 0.58	4.75		<0.001a
Tree BAI	Medium	-0.54 ± 0.10	-5.38		<0.001b
Tre	High	-0.47 ± 0.09	-5.00		<0.001b
AI	Low	0.002 ± 0.001	4.05		<0.001a
Stand BAI	Medium	-0.005 ± 0.001	-4.57		<0.001b
Stan	High	-0.009 ± 0.002	-4.03		<0.01 ^b
	Low				
NDVI	Medium	0.003 ± 0.001	5.36		< 0.001
	High				

Table 2. Average (± standard error) variables summarized by density category. Bolded variables were significantly different (P<0.05) among density categories. Superscript letters represent differences between categories. See Table S4 for linear mixed effect model results of the effect of density category on tree growth, stand productivity, and NDVI.

		Density Category	y			
Variable	Low	Medium	High	d.f.	F-value	P-value
Age (years)	53 ± 5.3	57 ± 4.0	60 ± 1.2	2,16	0.63	0.53
Density (stems ha ⁻¹)	1316.67 ± 468.63^{a}	5857.14 ± 613.68^{a}	21416.67 ± 4469.93^{b}	2,16	17.32	< 0.001
Tree Diameter (cm)	4.72 ± 0.39^a	4.03 ± 0.39^{ab}	3.04 ± 0.37^b	2,16	4.51	0.03
Basal Area (m ² ha ⁻¹)	3.19 ± 1.01^a	10.98 ± 1.47^{b}	18.75 ± 1.30^{c}	2,16	33.71	< 0.001
Canopy Cover (%)	18.11 ± 5.58^a	41.48 ± 5.28^{b}	70.17 ± 5.67^{c}	2,16	21.25	< 0.001
Active Layer Depth (cm)	72.79 ± 8.01^{a}	52.96 ± 3.24^{b}	53.65 ± 2.06^{b}	2,16	5.02	0.02
Soil Organic Layer Depth (cm)	11.15 ± 1.15	10.67 ± 0.74	10.17 ± 0.86	2,16	0.27	0.77
Total Tree (Mg C ha ⁻¹)	3.44 ± 1.11^{a}	11.61 ± 1.68^{b}	$19.90 \pm 1.31^{\circ}$	2,16	31.54	< 0.001
Total Understory (Mg C ha ⁻¹)	4.23 ± 0.74^a	2.46 ± 0.41^{ab}	1.23 ± 0.23^{b}	2,16	8.66	0.002
Total Aboveground (Mg C ha ⁻¹)	7.67 ± 1.34^a	14.07 ± 1.39 b	$21.13 \pm 1.31^{\circ}$	2,16	23.33	< 0.001
Tree growth (BAI; mm ² year ⁻¹)	$96.2 \pm 2.84^{\text{ a}}$	68.6 ± 1.88 a	31.00 ± 0.97 a	-	-	< 0.05
Stand productivity (BAI; m ² ha ⁻¹ y ⁻¹)	$0.08\pm0.005\mathrm{a}$	0.35 ± 0.01 b	0.63 ± 0.03 c	-	-	< 0.001
NDVI	0.73 ± 0.002 a	0.74 ± 0.001 b	0.72 ± 0.001 a	_	-	< 0.001

Table 3. Marginal mean estimates of the effect of seasonal climate variables on tree growth (basal area increment; mm^2 year⁻¹). Letters represent significant differences between density categories based on Tukey adjusted post-hoc pairwise comparisons (P<0.05). Note that model was fit on centered and scaled predictor variables and a natural log transformed response variable, but the estimated effect sizes presented here are on the original scale. Shaded cells represent a significant slope (P <0.05); red indicates a negative effect and grey indicates a positive effect. See Table S5 for the full model and Table S6 for reduced model results (marginal R^2 =0.16; conditional R^2 =0.83).

		Density Class				
	Season Climate Variable	Low	Medium	High		
	Previous Spring	2.25 a	-2.38 b	-1.21 b		
g.	Previous Growing Season		-1.02			
Temperature	Previous Fall	10.96 a	-0.20 b	-1.20 b		
	Winter	0.82 a	2.03 a	1.21 a		
Te	Current Spring	0.34 a	-3.25 b	-1.35 °		
	Current Growing Season	8.34 a	3.12 b	0.20 °		
	Previous Spring	-1.83 a	-0.12 b	0.06 b		
u u	Previous Growing Season	-0.23 a	0.15 b	0.13 b		
Precipitation	Previous Fall	0.33 a	0.10 b	0.05 b		
	Winter	-0.13 ^a				
Pr	Current Spring	-1.84 a	0.44 b	0.38 b		
	Current Growing Season		0.03			

Figure Legends

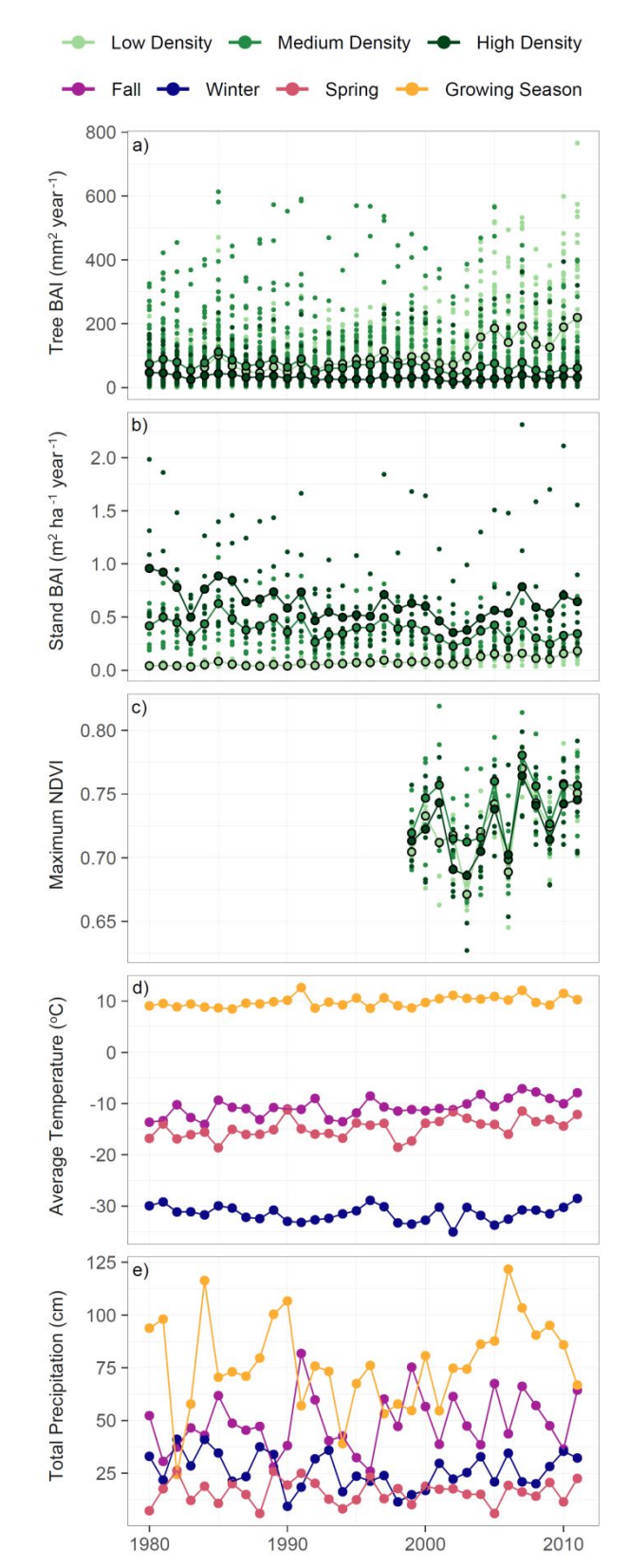
Fig. 1. Averages over the study period (1980-2011) in a) tree productivity (mm² year¹) measured as annual basal area increment (BAI), b) stand level productivity (m² ha⁻¹ year⁻¹) calculated as mean annual BAI per stand multiplied by tree density, c) annual maximum normalized difference vegetation index (NDVI) obtained from Landsat, and seasonal d) average temperature (°C) and e) total precipitation (mm) (represented by different colors). In a), b), and c) lines and large points represent means associated with each density category (low=light green, medium=green, and high=dark green), and smaller points represent individual tree (a) or stand (b, c) values. See Table 1 and Table S3 for the statistical results of trends in these parameters over the study period.

Fig. 2. Tree growth (mm² year⁻¹), measured as annual basal area increment (BAI), correlations to monthly temperatures and precipitation in low, medium, and high density stands. Months in lowercase represent the year prior to ring formation and uppercase represent the year of ring formation. Large points represent the mean correlation and small points represent individual tree correlation. All colored points are significant (P<0.05).

Fig. 3. Annual maximum normalized difference vegetation index (NDVI) from Landsat as a function of stand productivity (m² ha⁻¹ year⁻¹), calculated as mean basal area increment per stand multiplied by density, over the time period 1999-2011. Lines represents model fitted relationships with shading over the 95% confidence interval from a linear mixed effects model with stand as a random effect. Solid lines represent a significant (P<0.05) effect. See Table S7 for model results.

838

839 Fig. 1. Averages over the study period (1980-2011) in a) tree productivity (mm² year⁻¹) 840 measured as annual basal area increment 841 842 (BAI), b) stand level productivity (m² ha⁻¹ year 1) calculated as mean annual BAI per stand 843 multiplied by tree density, c) annual maximum 844 normalized difference vegetation index (NDVI) 845 obtained from Landsat, and seasonal d) average 846 temperature (°C) and e) total precipitation 847 (mm) (represented by different colors). In a), 848 b), and c) lines and large points represent 849 850 means associated with each density category (low=light green, medium=green, and 851 high=dark green), and smaller points represent 852 individual tree (a) or stand (b, c) values. See 853 Table 1 and Table S3 for the statistical results 854 of trends in these parameters over the study 855 period. 856



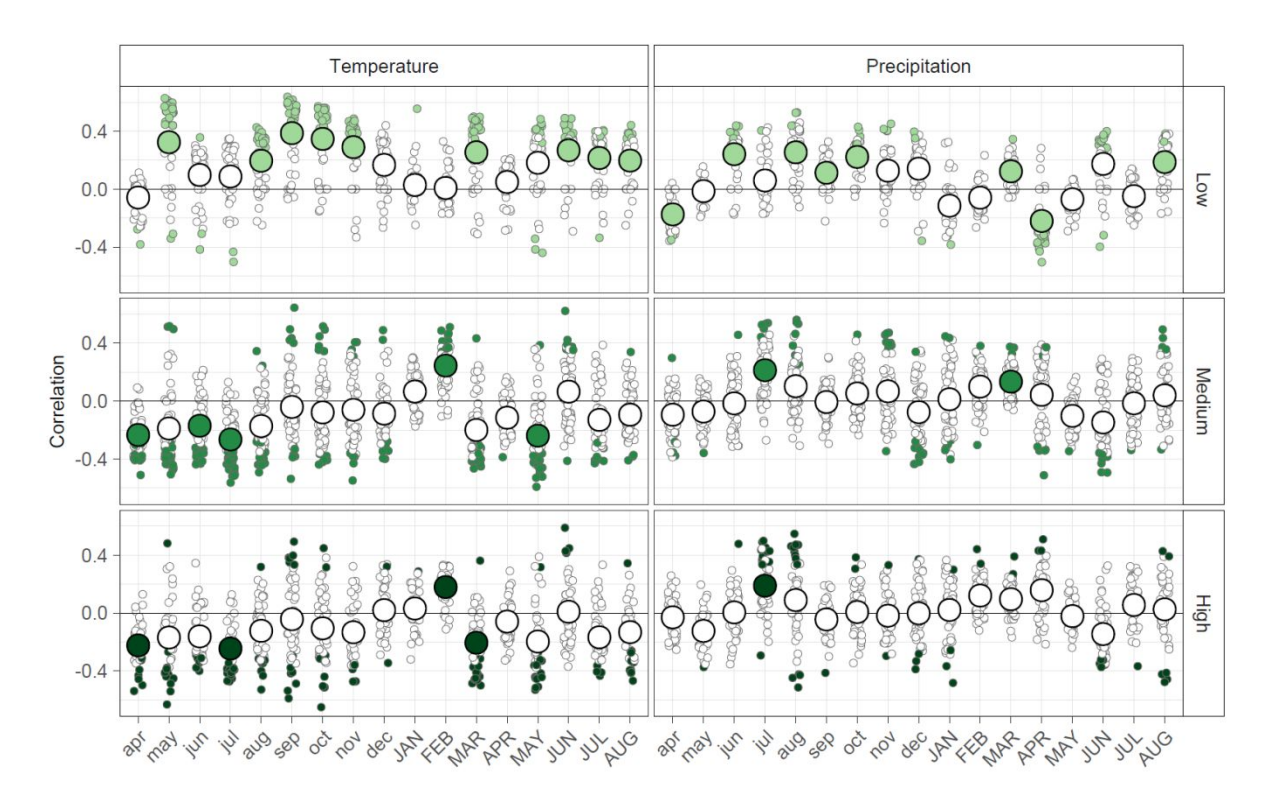


Fig. 2. Tree growth (mm² year¹), measured as annual basal area increment (BAI), correlations to monthly temperatures and precipitation in low, medium, and high density stands. Months in lowercase represent the year prior to ring formation and uppercase represent the year of ring formation. Large points represent the mean correlations and small points represent individual tree correlations. All colored points are significant (P<0.05).

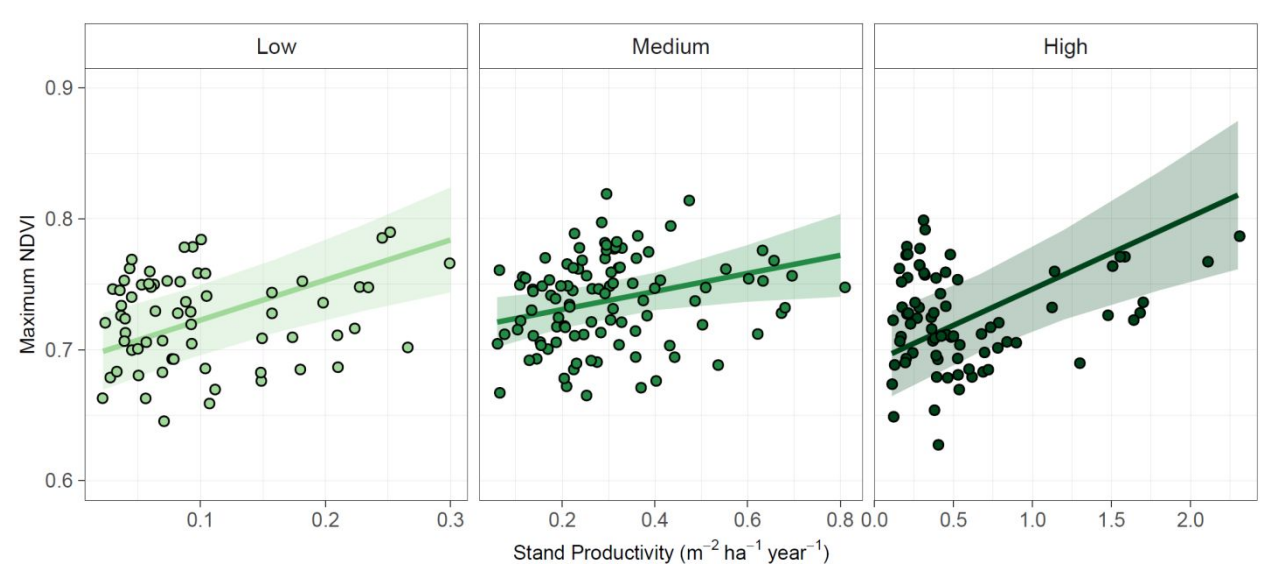


Fig. 3. Annual maximum normalized difference vegetation index (NDVI) from Landsat as a function of stand level productivity (m² ha⁻¹ year⁻¹), calculated as mean basal area increment per stand multiplied by density, over the time period 1999-2011 for each density category (low, medium, high). Lines represents model fitted relationships with shading over the 95% confidence interval from a linear mixed effects model with stand as a random effect. Solid lines represent a significant (P<0.05) effect. Note the difference in x-axes between panels. See Table S7 model results.

Appendix: Sensitivity analysis of linear mixed model correlation structures and detrending method

Annual trends in growth, productivity, and NDVI with modeled autocorrelation

To assess temporal changes in tree growth (mm² year-¹) and stand productivity (m² ha-¹ year-¹) from 1980-2011 and NDVI from 1999-2011 we fit linear mixed effects models (LMM) using the package 'nlme' (Pinheiro et al. 2017). LMM can account for hierarchical sampling, temporal autocorrelation, and unbalanced sampling design (Zuur et al. 2009). The use of LMM for tree ring analyses is becoming increasingly common because they can account for the variance in growth between years within individual trees, the variance between individuals within sites, as well as the variance in growth over time for trees located in the same site.

In the main text we modelled each of tree BAI, stand BAI, and NDVI with fixed effects of year, stand density category (low, medium, or high), and their interaction. We natural log transformed tree BAI and stand BAI prior to analysis. For the response variable of tree BAI, we included random intercepts for site and tree nested within site to account for the spatial nonindependence of trees within sites and the non-independence of annual BAI measurements within a tree. For the response variables of stand BAI and NDVI, we included stand as a random intercept to account for the non-independence of measurements within a site. To confirm that our choice of random intercepts was accounting for the temporal non-independence of measurements in time series of BAI and NDVI we compared these models with models that included an autocorrelation structure. For the response variable of tree BAI, we included random intercepts for site and year nested within site and an autocorrelation structure (AR1, autoregressive process of order one) to account for the temporal non-independence of annual BAI measurements within a tree and the spatial non-independence of trees within sites. For the response variable of stand BAI and NDVI, we included the random intercept of year and an autocorrelation structure (AR1) to account for the temporal non-independence of measurements. We could not include random intercepts of tree nested within site (for the tree BAI model) or site (for site BAI and NDVI) in addition to a random intercept of year and AR1 because this results in only one observation per hierarchical random effect and as such models failed to converge. We compared models using Akaike information criterion (AIC), where a lower AIC indicates a better model fit. In all cases, the inclusion of a random intercept for year and AR1 substantially increased AIC (Table A1), but produced very similar results (Table A2) to the models we present in the main text (Table 1).

Table A1. Akaike information criterion (AIC) for models that included an autoregressive structure (AR1, autoregressive process of order one) and random intercepts for site and year nested within site (for the tree BAI model) or year (for site BAI and NDVI model) compared to AIC for models with random intercepts for site and tree (for the tree BAI model) or random intercepts for site (for site BAI and NDVI).

	AR1 included	AR1 not included
		(models in main text)
Tree BAI	12899.56	7037.14
Site BAI	1017.75	362.12
NDVI	-1001.13	-1033.51

Table A2. Modeled slope estimates and standard errors of tree growth, site productivity, and NDVI as a function of year for low, medium, and high density sites. Tree growth and stand productivity were natural log transformed prior to analysis but effect sizes are on the original scale. Group letters represent significant (P<0.05) differences between the slopes of the three density categories as determined by Tukey adjusted post-hoc pairwise comparisons. For NDVI, there was no interaction between year and NDVI, thus only one value is presented. Red text indicates a negative trend and black indicates a positive trend. Shaded cells represent a significant effect.

Model		Effect ± st.error	t-value	p-value	group
vth	Low	2.68 ± 0.55	4.86	< 0.001	a
Tree growth	Medium	-0.55 ± 0.13	-4.40	< 0.001	b
Tree	High	-0.48 ± 0.10	-4.66	< 0.001	b
ity	Low	0.002 ± 0.0003	6.52	< 0.001	a
Stand productivity	Medium	-0.004 ± 0.001	-3.03	< 0.05	b
	High	-0.009 ± 0.003	-3.26	< 0.05	b
	Low				
NDVI	Medium	0.003 ± 0.002	1.70	0.12	
	High				

Climate growth analysis with modeled autocorrelation

To assess the effects of seasonal climate and stand density on tree growth we fit LMM. We used natural log transformed individual tree BAI as the response variable and fixed effects of seasonal mean temperature and total precipitation and the first order interaction with tree density category (low, medium, high). We scaled and centered all continuous climate predictor variables prior to model fitting. In the main text, we included random intercepts for stand and tree nested within stand. Here, we fit the model with AR1 and a random intercept of site and year nested within site. This substantially increased the AIC of the full model (13379 with AR1 vs. 7311 without), but produced very similar results (Table A3).

Table A3. Marginal mean estimates of the effect of seasonal climate variables on tree growth (BAI; mm² year⁻¹) based on a linear mixed effects model with the random effects of stand and year nested within stand and an autocorrelation structure (AR1, autoregressive process of order one). Letters indicate differences (P < 0.05) between density classes based on Tukey adjusted post-hoc pairwise comparisons. Note that model was fit with centered and scaled predictor variables and a natural log transformed response variable, but the estimated effect sizes presented here are on the original scale. Shaded cells represent a significant slope (P < 0.05); red indicates a negative effect and grey indicates a positive effect (marginal $R^2=0.16$; conditional $R^2=0.35$).

		Density Class				
	Season Climate Variable	Low	Medium	High		
	Previous Spring	1.98 a	-2.36 b	-1.20 b		
မ	Previous Growing Season		-1.02			
ratu	Previous Fall	10.84 a	-0.29 b	-1.25 b		
Temperature	Winter	1.64				
Te	Current Spring	-0.23 a	-3.16 a	-1.26 a		
	Current Growing Season	9.66 a	2.76 ab	-0.10 b		
	Previous Spring	-1.65 a	-0.17 b	0.03 b		
l u	Previous Growing Season	-0.23 a	0.15 b	0.14 b		
Precipitation	Previous Fall	0.13				
ecipi	Winter	-0.13				
Pro	Current Spring	-1.84 a	0.46 b	0.39 b		
	Current Growing Season		0.03			

Climate growth analyses with different detrending methods

In order to assess the effects of climate on tree growth, age related trends need to be removed from raw ring width series. There are a variety of methods that can be used to complete this detrending process. Here, we detrended our raw ring width series using the C-method and a modified negative exponential approach. We also prewhitened basal area increment (BAI) chronologies to remove autocorrelation. This is acommon practice for climate growth analyses but can distort the information content of the time series (Razavi and Vogel 2018) and is not recommended when assessing correlations with previous year climate(Zang and Biondi 2013). Detrending and prewhitening was completed in the R package 'dplR' (Bunn 2010). The full length of each individual tree ring series was detrended or prewhitened. We present chronologies for stand density categories of low, medium, and high (Figure A1) and chronology statistics (Table A4) during the period in which we assessed productivity responses to climate (1980-2011). Analyses were completed on individual trees.

For each of the detrended or prewhitened chronologies we assessed productivity responses to climate over the period 1980-2011 using two methods. We first calculated bootstrapped correlations between individual tree chronologies and mean monthly temperatures and total monthly precipitation over a 17-month climate window, extending from April of the year preceding growth to August of the current year of growth (Fritts 1976), using the package 'bootRes, version 1.2.3' (Zang 2010). The significance of the 34 climate correlations were determined from 95% confidence intervals (Zang 2010). These monthly correlations were done at the individual tree level in order to maintain the variation associated with each tree. Because we were interested in the effect of stand density on climate growth responses, we grouped trees based on stand density category (low, medium, high) and created plots showing the mean correlation and its significance based on a 95% confidence interval for each of the 34 monthly climate variables.

In addition to the descriptive monthly correlation analysis, we fit LMM to determine the effects of seasonal climate and stand density on tree productivity. Seasonal climate parameters were used instead of monthly due to collinearity of monthly variables. We used natural log transformed individual tree BAI chronologies as the response variable and fixed effects of seasonal mean temperature, total precipitation, stand density category (low, medium, high), and the first order interaction between temperature or precipitation and stand density category. We included stand and tree nested within stand as random effects. For each of the seasonal climate parameters that significantly interacted with density class, we tested for the significance of each density class slope and used a Tukey adjusted post hoc analysis for pairwise comparisons of slopes between the density classes in the 'emmeans' package (Lenth, Singmann, Love, Buerkner & Herve, 2019).

We found that raw ring widths (Figure A2 and Table A5), pre-whitened BAI (Figure A3 and Table A6), the C-method (Figure A4 and Table A7), and the modified negative exponential approach (Figure A5 and Table A8) produced similar results to the BAI chronologies we present in the main text.

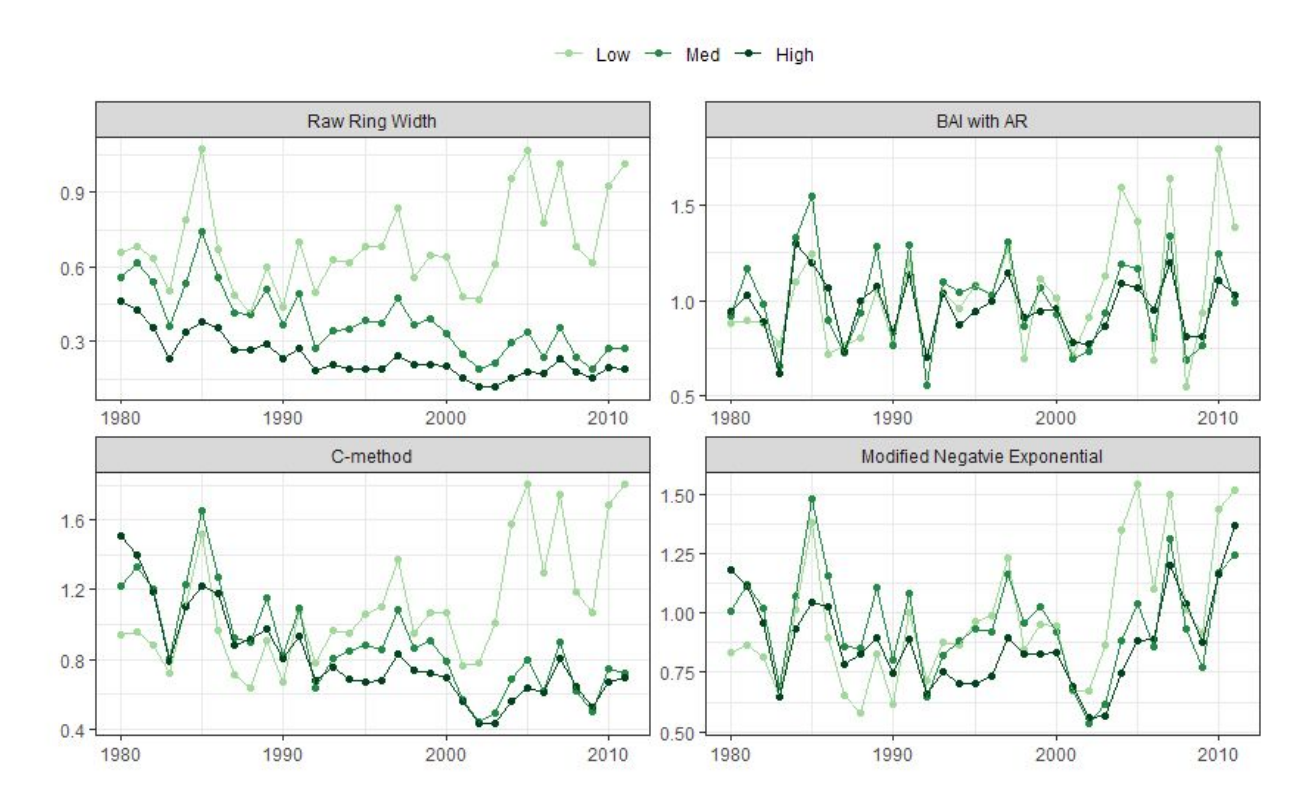


Figure A1. Raw ring width, prewhitened BAI (BAI with AR), and detrended raw ring width chronologies using the C-method and a modified negative exponential approach over the study period (1980-2011). Lines and points represent means associated with each density category (low=light green, medium=green, and high=dark green).

Table A4. The number of trees within each density category and statistics of mean series intercorrelation (IC), autocorrelation (AR), effective signal (Rbar eff), expressed population signal (EPS), and the signal-to-noise ratio for each detrending method.

Detrending	Density	#	IC		Rbar		
Method	Class	trees	(st.dev)	AR (st.dev)	eff	EPS	SNR
Raw Ring Widths	Low	40	0.63 (0.15)	0.49 (0.19_	0.291	0.942	16.28
Widiis	Med	63	0.69 (0.15)	0.58 (0.16)	0.547	0.987	76.14
	High	47	0.48 (0.25)	0.61 (0.16)	0.487	0.978	44.53
BAI with	Low	40	0.67 (0.18)	-0.13 (0.15)	0.499	0.975	39.19
Auto- regressive	Med	63	0.67 (0.16)	-0.14 (0.13)	0.468	0.982	55.24
	High	47	0.48 (0.29)	-0.14 (0.14)	0.228	0.933	13.87
C-method	Low	40	0.65 (0.15)	0.52 (0.19)	0.334	0.950	19.93
	Med	63	0.69 (0.13)	0.56 (0.16)	0.484	0.983	59.07
	High	47	0.49 (0.25)	0.59 (0.16)	0.422	0.972	34.28
Modified	Low	40	0.65 (0.14)	0.47 (0.21)	0.352	0.956	21.52
Negative Exponential	Med	63	0.64 (0.14)	0.41 (0.20)	0.333	0.969	31.41
	High	47	0.46 (0.26)	0.52 (0.19)	0.222	0.931	13.41

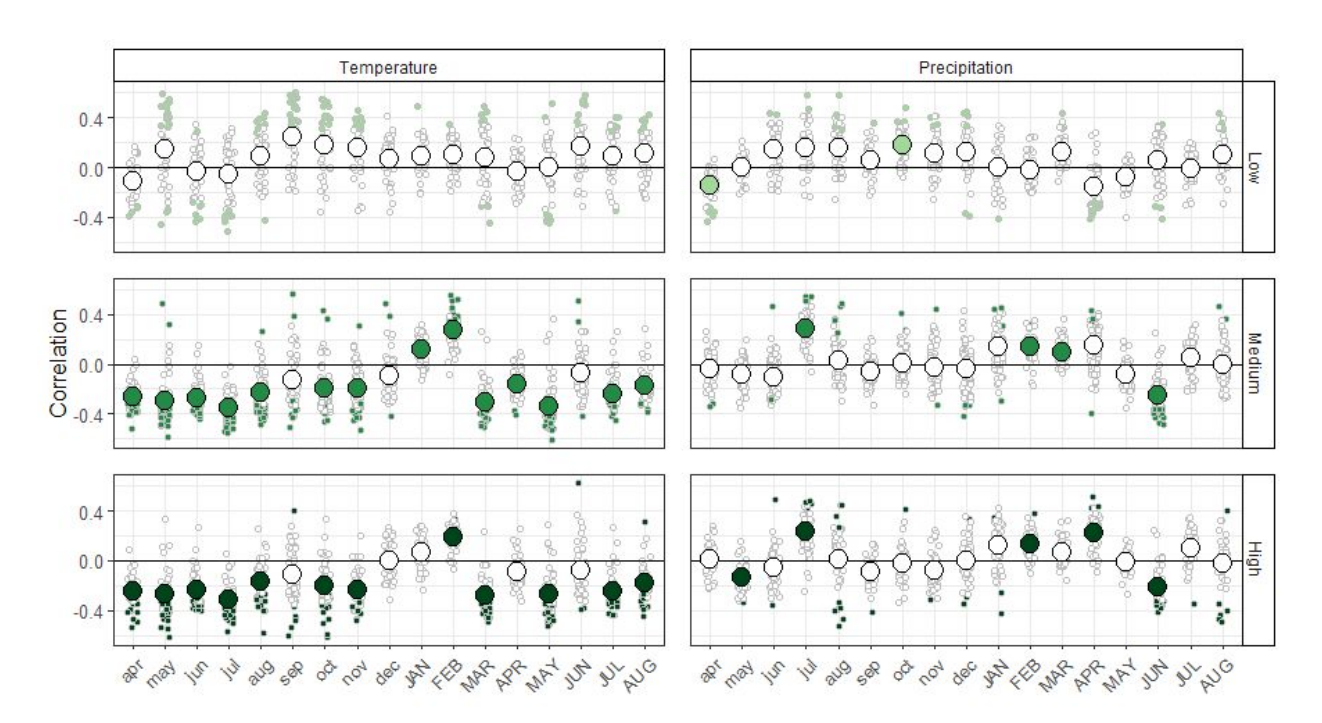


Figure A2. Raw ring width correlations to monthly temperatures and precipitation in low, medium, and high-density stands. Months in lowercase represent the year prior to ring formation and uppercase represent the year of ring formation. Large points represent the mean correlation and small points represent individual tree correlations. All colored points are significant (p<0.05).

Table A5. Marginal mean estimates of the effect of seasonal climate variables on raw ring width (mm) based on a linear mixed effects model with the random effects of stand and tree nested within stand. Letters indicate differences (p <0.05) between density classes based on Tukey adjusted post-hoc pairwise comparisons. Note that model was fit on centered and scaled predictor variables and a natural log transformed response variable, but the estimated effect sizes presented here are on the original scale. Shaded cells represent a significant slope (p <0.05); red indicates a negative effect and grey indicates a positive effect (marginal R^2 =0.34; conditional R^2 =0.76).

			Density Class	
	Season Climate Variable	Low	Medium	High
	Previous Spring	0.00 a	-0.02 b	-0.01 ^b
ure	Previous Growing Season		-0.01	
rat	Previous Fall	0.03 a	-0.02 b	-0.02 °
Temperature	Winter			
	Current Spring	-0.02 a	-0.03 b	-0.02 b
L	Current Growing Season	0.05 a	0.01 b	-0.15 °
	Previous Spring	-0.01 a	0.002 b	0.002 b
ion	Previous Growing Season	-0.00 a	0.002 b	0.001 b
itat	Previous Fall	0.004 a	0.00 b	0.00 b
cip	Winter	0.00 a	-0.001 a	0.00 a
Precipitation	Current Spring	-0.004 a	0.01 b	0.004 b
_ '	Current Growing Season		0.001	

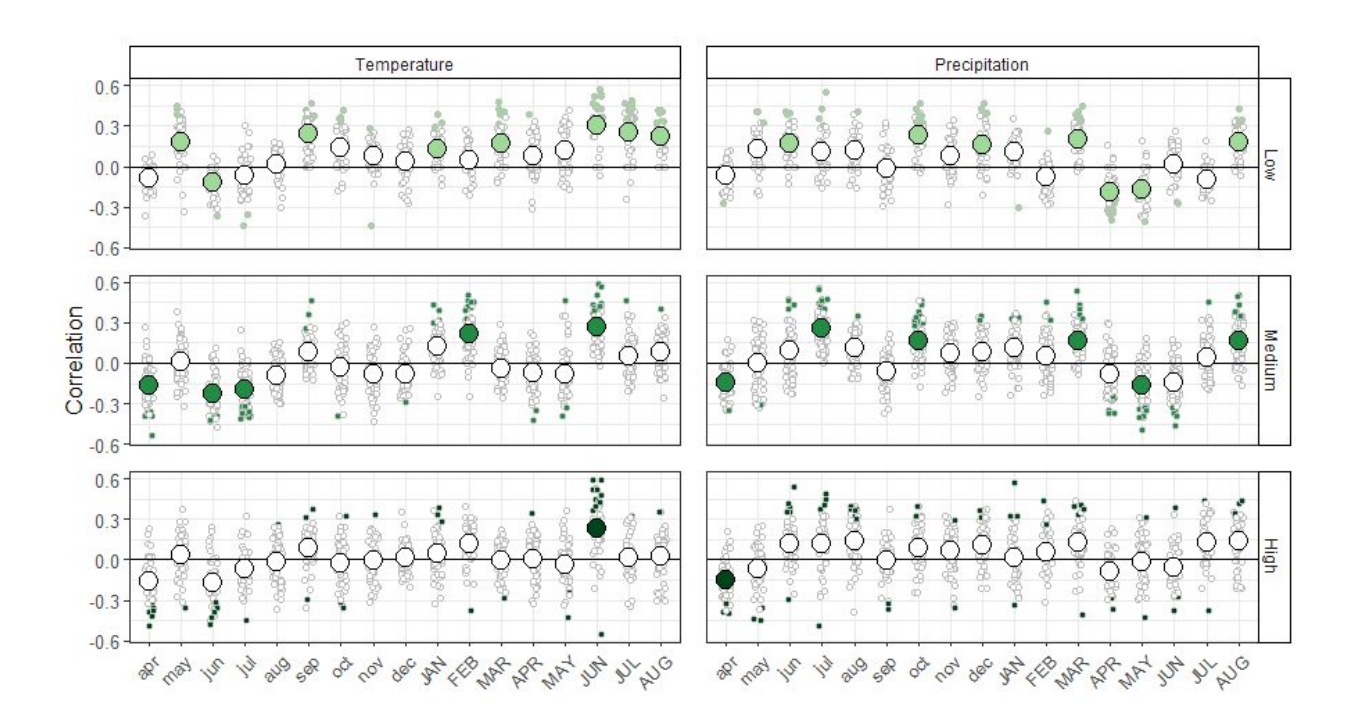


Figure A3. Prewhitened basal area increment correlations to monthly temperatures and precipitation in low, medium, and high-density stands. Months in lowercase represent the year prior to ring formation and uppercase represent the year of ring formation. Large points represent the mean correlation and small points represent individual tree correlations. All colored points are significant (p<0.05).

Table A6. Marginal mean estimates of the effect of seasonal climate variables on prewhitened basal area increment chronologies based on a linear mixed effects model with the random effects of stand and tree nested within stand. Letters indicate differences (P < 0.05) between density classes based on Tukey adjusted post-hoc pairwise comparisons. Note that model was fit on centered and scaled predictor variables, but the estimated effect sizes presented here are on the original scale. Shaded cells represent a significant slope (P < 0.05); red indicates a negative effect and grey indicates a positive effect (marginal $R^2 = 0.20$); conditional $R^2 = 0.20$).

		Density Class			
	Season Climate Variable	Low	Medium	High	
	Previous Spring		-0.01		
ure	Previous Growing Season		-0.05		
erat	Previous Fall	0.06 a	0.003 в	0.01 b	
Temperature	Winter	0.03			
 	Current Spring	-0.01 a	-0.05 b	-0.03 ab	
	Current Growing Season	0.18 a	0.12 b	0.08 °	
	Previous Spring		-0.01		
10n	Previous Growing Season	-0.001 a	0.002 b	0.001 b	
itat	Previous Fall	0.002			
Precipitation	Winter	0.01 a	0.002 в	0.0002 b	
	Current Spring	-0.01 a	0.001 b	0.003 b	
	Current Growing Season	-0.001 a	0.001 ab	0.002 b	

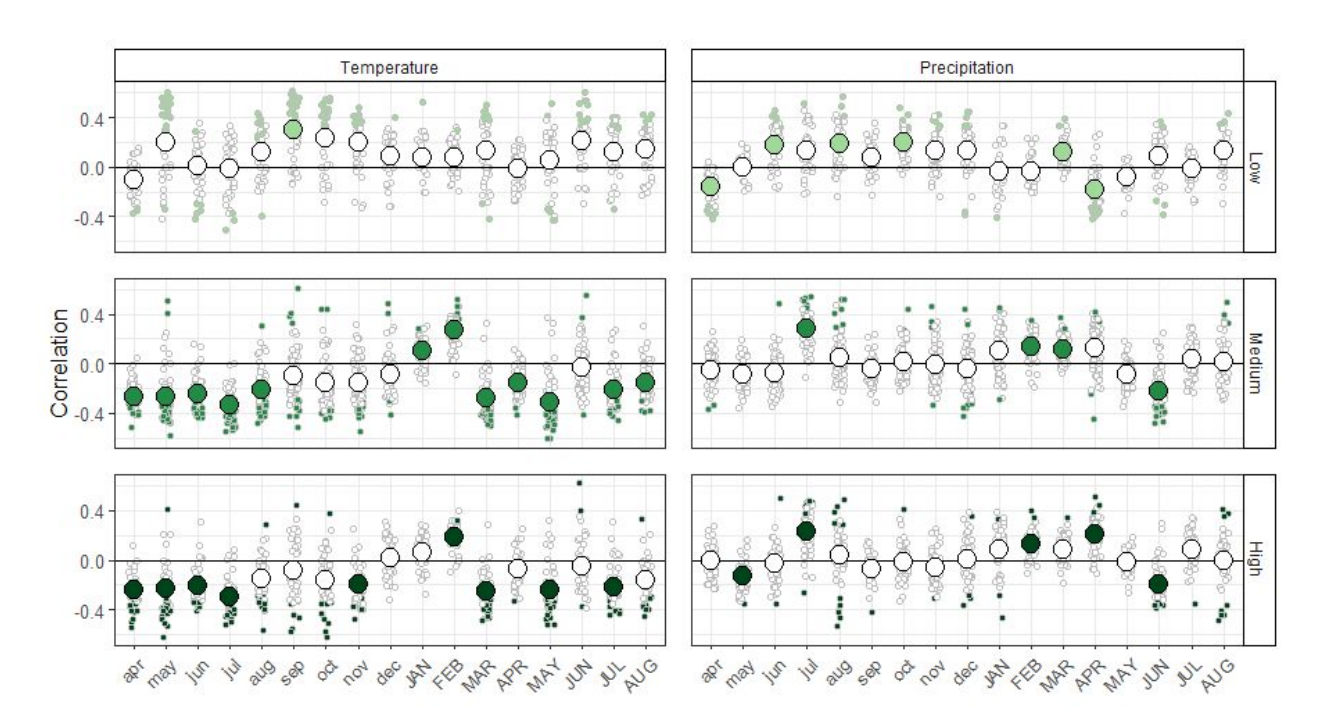


Figure A4. Correlations between detrended ring width series using the C-method to monthly temperatures and precipitation in low, medium, and high-density stands. Months in lowercase represent the year prior to ring formation and uppercase represent the year of ring formation. Large points represent the mean correlation and small points represent individual tree correlations. All colored points are significant (p<0.05).

Table A7. Marginal mean estimates of the effect of seasonal climate variables on detrended ring width series using the C-method based on a linear mixed effects model with the random effects of stand and tree nested within stand. Letters indicate differences (P < 0.05) between density classes based on Tukey adjusted post-hoc pairwise comparisons. Note that model was fit on centered and scaled predictor variables and a natural log transformed response variable, but the estimated effect sizes presented here are on the original scale. Shaded cells represent a significant slope (P < 0.05); red indicates a negative effect and grey indicates a positive effect (marginal $R^2 = 0.29$; conditional $R^2 = 0.47$).

		Density Class			
	Season Climate Variable	Low	Medium	High	
45	Previous Spring	0.01 a	-0.05 b	-0.04 b	
Temperature	Previous Growing Season		-0.03		
rat	Previous Fall	0.08 a	-0.04 b	-0.06 b	
ube	Winter	0.06			
Ter	Current Spring	-0.03 a	-0.08 b	-0.05 °	
	Current Growing Season	0.10 a	0.03 b	-0.02 °	
	Previous Spring	-0.02 a	0.003 b	0.005 b	
10n	Previous Growing Season	-0.001 a	0.01 b	0.01 b	
itat	Previous Fall	0.01 a	0.001 b	0.001 b	
Precipitation	Winter	0.00 a	-0.003 b	-0.00 ab	
	Current Spring	-0.01 a	0.01 b	0.02 b	
	Current Growing Season		0.002		

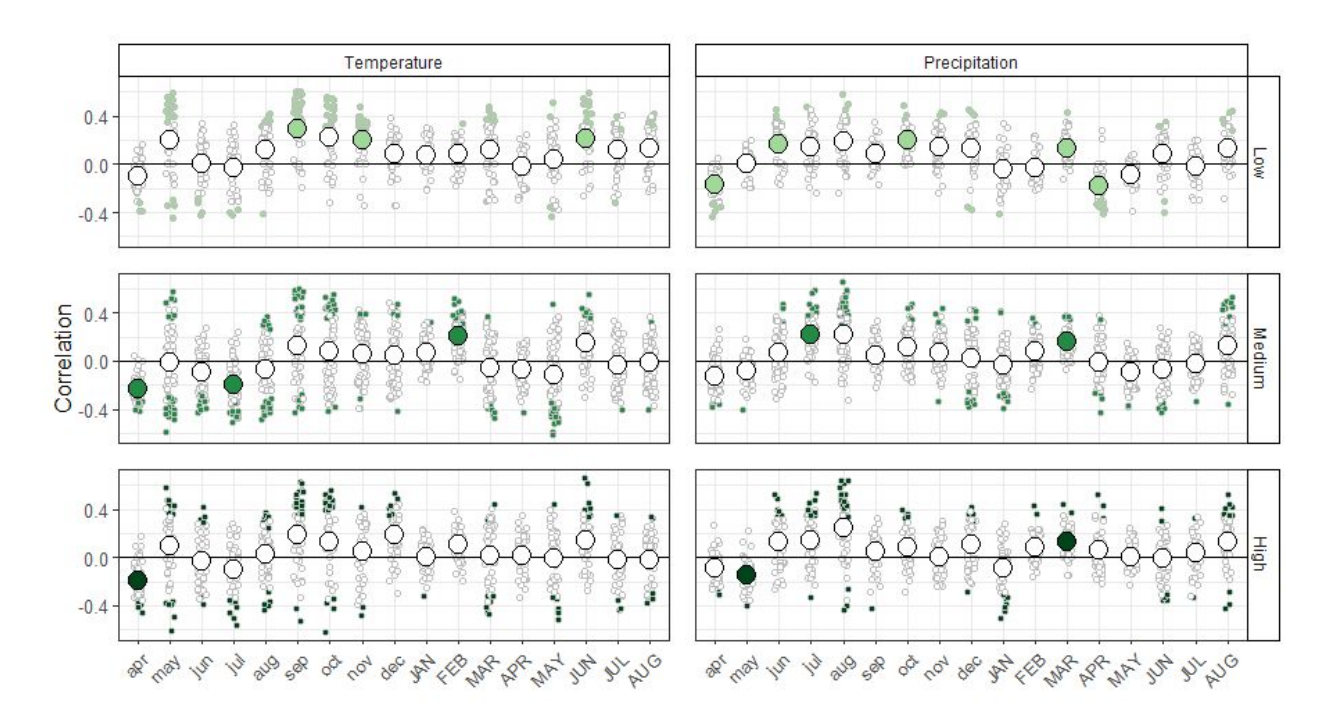


Figure A5. Correlations between detrended ring width series using the modified negative exponential method to monthly temperatures and precipitation in low, medium, and high-density stands. Months in lowercase represent the year prior to ring formation and uppercase represent the year of ring formation. Large points represent the mean correlation and small points represent individual tree correlations. All colored points are significant (p<0.05).

Table A8. Marginal mean estimates of the effect of seasonal climate variables on detrended ring width series using the modified negative exponential method based on a linear mixed effects model with the random effects of stand and tree nested within stand. Letters indicate differences (p <0.05) between density classes based on Tukey adjusted post-hoc pairwise comparisons. Note that model was fit on centered and scaled predictor variables and a natural log transformed response variable, but the estimated effect sizes presented here are on the original scale. Shaded cells represent a significant slope (p <0.05); red indicates a negative effect and grey indicates a positive effect (marginal R^2 =0.16; conditional R^2 =0.40).

		Density Class			
	Season Climate Variable	Low	Medium	High	
	Previous Spring	0.001 a	-0.03 b	-0.02 ab	
ure	Previous Growing Season		-0.03		
	Previous Fall	0.08 a	0.02 b	-0.001 ^b	
Temperature	Winter 0.05				
ler	Current Spring	-0.04 a	-0.05 b	-0.03 ab	
	Current Growing Season	0.10 a	0.06 a	-0.001 ^b	
	Previous Spring	-0.01 a	-0.01 ab	-0.01 b	
10n	Previous Growing Season	-0.001 a	0.00 b	0.004 b	
itat	Previous Fall		0.004		
cip	Winter		-0.001		
Precipitation	Current Spring	-0.01 a	0.004 b	0.004 b	
	Current Growing Season		0.001		

References

- Fritts, H.C. 1976. Tree Rings and Climate. Academic Press, London.
- Lenth, R., Singmann, H., Love, J., Buerkner, P., and Herve, M. 2019. emmeans: Estimated Marginal Means, aka Least-Squares Means. Available from https://CRAN.R-project.org/package=emmeans [accessed 18 April 2019].
- Pinheiro, J., Bates, D., DebRoy, S., Sarkar, D., Heisterkamp, S., Van Willigen, B., and Maintainer, R. 2017. Package 'nlme.' Linear and Nonlinear Mixed Effects Models, version: 3–1.
- Razavi, S., and Vogel, R. 2018. Prewhitening of hydroclimatic time series? Implications for inferred change and variability across time scales. Journal of Hydrology **557**: 109–115. doi:10.1016/j.jhydrol.2017.11.053.
- Zang, C. 2010. bootRes: Bootstrapped response and correlation functions. R package version 0.3. http://cran.r-project.org/web/packages/bootRes/.
- Zang, C., and Biondi, F. 2013. Dendroclimatic calibration in R: The bootRes package for response and correlation function analysis. Dendrochronologia **31**(1): 68–74. doi:10.1016/j.dendro.2012.08.001.
- Zuur, A., Ieno, E.N., Walker, N., Saveliev, A.A., and Smith, G.M. 2009. Mixed effects models and extensions in ecology with R. Springer Science & Business Media.